

## Ye'elimite synthesis by chemical routes

Y. EL KHESSAIMI, Y. EL HAFIANE, A. SMITH \*

IRCER, UMR CNRS 7315, Université de Limoges, Centre Européen de la Céramique, 12 avenue Atlantis, 87068 Limoges cedex.

\* Corresponding author: [agnes.smith@unilim.fr](mailto:agnes.smith@unilim.fr)

### Summary and novel conclusions

- Complete and detailed description for the synthesis of orthorhombic ye'elimite by chemical routes: Pechini method, organic steric entrapment method, self-propagation combustion method.
- A heat treatment at 1250 °C for 1 h is sufficient to obtain pure ye'elimite.
- The final powder contains agglomerates whose size range between 1 to 100 µm, which is typical of a ground Portland clinker or cement.
- The present work provide an original protocol to synthesize nano-sized ye'elimite particles with very small crystallite size by chemical routes. This ye'elimite could be usefully exploited for hydration studies.
- Compared to a Portland cement, the lower sintering temperature (1250 °C instead of 1450 °C) and the absence of grinding implies energy savings in the manufacturing process.

### Abstract

Ye'elimite is formed during the production of sulfoaluminate cement. This article presents the synthesis of ye'elimite by different chemical routes: Pechini method (Pech), Organic Steric Entrapment method (OSE) and Self-Propagating Combustion (SPC). 1250 °C for 1 hour is the

optimal sintering cycle to synthesize ye'elimite, which is lower than the sintering conditions (1300 °C, 3 h) to obtain pure ye'elimite from solid-state reaction using pure oxide raw materials. OSE and SPC methods produce the purest ye'elimite (> 98 wt%). After the heat treatment, the nanosized crystallites (51 to 57 nm) form particles about 3 times larger (136 to 175 nm) which could result from the sintering of the crystallites. The particles form hard agglomerates whose size ranges between 1 to 100 µm. This distribution, which is typical of a ground Portland clinker, is obtained in the present case directly after sintering and without the necessity of a grinding step.

Y. EL KHESSAIMI, Y. EL HAFIANE, A. SMITH \*

IRCER, UMR CNRS 7315, Université de Limoges, Centre Européen de la Céramique, 12 avenue Atlantis, 87068 Limoges cedex.

\* Corresponding author: agnes.smith@unilim.fr

### 1. Introduction

Calcium Sulfoaluminate Cement (CSA) presents a promising alternative to Ordinary Portland Cement (OPC) in view of sustainable development [1]. The production of CSA clinker involves less embodied energy and CO<sub>2</sub> emissions compared to the OPC cement, because CSA clinker requires less limestone, a lower grinding energy and a lower clinkering temperature than OPC clinker. Ye'elimite (Ca<sub>4</sub>Al<sub>6</sub>O<sub>16</sub>S or C<sub>4</sub>A<sub>3</sub> $\bar{S}$ )\* is the main phase of CSA clinker [2–7]. To study and explain the hydration behaviour of calcium sulfoaluminate cements, individual and pure components should be prepared, one of which is ye'elimite. As commercially available CSA cements are a mix of several phases, it is impossible to separate ye'elimite from the other phases. Therefore, a need exists to synthesize C<sub>4</sub>A<sub>3</sub> $\bar{S}$  phase in a pure state at the lab scale.

When ye'elimite is prepared by solid-state reactions, the final product contains phases like krotite (CA), grossite (CA<sub>2</sub>) and mayenite (C<sub>12</sub>A<sub>7</sub>) as secondary phases below 1300 °C. Hence, successful preparation of C<sub>4</sub>A<sub>3</sub> $\bar{S}$  by solid state reaction required intermediate grinding steps and high-temperature firings (at or above 1300 °C) [2–7].

Nowadays, it is possible to bypass the grinding and refiring steps and to decrease the synthesis temperature of cementitious pure phases through chemical routes starting from a solution. According to the literature, different polymer precursor methods were used in this case. Polymer precursor methods such as Pechini method (Pech), Organic Steric Entrapment method

---

\* The cement phase notations are used in this work (C= CaO, A = Al<sub>2</sub>O<sub>3</sub>, S=SiO<sub>2</sub>,  $\bar{S}$  = SO<sub>3</sub>,  $\bar{C}$  = CO<sub>2</sub>, H = H<sub>2</sub>O).

(OSE) and Self-Propagating Combustion (SPC) are well known for the synthesis of calcium aluminates and calcium silicates [8]. These chemical methods are based on the mixing of salts with a polymer precursor (citric acid, ethylene glycol or polyvinyl alcohol). The polymerization reaction progresses by increasing temperature. The solution was heated until the formation of a viscous gel was achieved. The gel was dried and a foam was formed. The foam was crushed and used as a precursor material for the subsequent sintering process [8].

Table 1 summarizes physical and chemical characteristics of some cementitious phases prepared by chemical synthesis routes [9–21]. Ye’elimite was prepared by Song et al. [9] using chemical synthesis from calcium nitrate, aluminum nitrate and aluminum sulfate. The specific surface area of the synthesized ye’elimite after calcination at 1300 °C was 1 m<sup>2</sup>.g<sup>-1</sup>. Lee and Kriven [10] were able to produce C<sub>3</sub>S, C<sub>2</sub>S, C<sub>3</sub>A and C<sub>4</sub>AF by an organic steric entrapment method. The cement components synthesized by chemical routes have sub-micronic or nanometric crystallites, high specific surface area and extremely high reactivity at relatively low calcination and crystallization temperatures. Raab and Pöllmann [11] synthesized pure phases of Portland and Calcium Aluminate Cements (CAC), with particle sizes around 50 nm, using the Pechini or the combustion method. Thomas et al. [12] managed to prepare highly reactive forms of β-C<sub>2</sub>S with specific surface areas of 8.3 m<sup>2</sup>.g<sup>-1</sup> and 26.5 m<sup>2</sup>.g<sup>-1</sup> using the Pechini method. There is also other work [13–15] on reactive forms of β-C<sub>2</sub>S synthesis by the Pechini process. Use of the self-propagating combustion method for preparation of clinker phases was reported by Zapata and Bosch [16], who synthesized C<sub>3</sub>S phase at low temperature, and by Fumo et al. [17], Tas [18] and Yi et al. [19], who synthesized calcium aluminate cementitious phases.

Referring to Table 1, there is only one work in literature which deals with ye’elimite synthesis by a chemical route [9]. The multiscale size characterization and the effect of organic precursors on ye’elimite synthesis were not investigated. The purity of the synthesized ye’elimite [9] was

not confirmed by accurate methods like Rietveld analysis when examination of pure cement phases requires knowledge of the purity. Detailed characterization of the microstructure is also important [22,23].

The present paper deals with the synthesis of pure orthorhombic ye'elimite using three low temperature chemical routes: Pech method, OSE method and SPC synthesis. The different synthesized products were compared in terms of purity and physical characteristics. The purity was deduced from Rietveld quantitative analysis. The physical characteristics were studied by Scanning Electron Microscopy, particle size analysis and X-Ray Diffraction. Finally, the dried gels were characterized by thermal analysis.

## 2. Experiments

### 2-1- Materials and methods

$\text{Ca}(\text{NO}_3)_2 \cdot 4\text{H}_2\text{O}$  (N°CAS: 13477-34-4, Fisher Scientific),  $\text{Al}(\text{NO}_3)_3 \cdot 9\text{H}_2\text{O}$  (N°CAS: 7784-27-2, Fisher Scientific) and  $\text{Al}_2(\text{SO}_4)_3 \cdot 16\text{H}_2\text{O}$  (N°CAS: 17927-65-0, Fisher Scientific) were used as starting materials and mixed in stoichiometric amounts corresponding to ye'elimite.

The steps and the amounts of raw materials for the synthesis of ye'elimite through the different chemical routes are presented in Fig. 1 and Table 2, respectively. Each method is described below. For each route, a schematic representation of the reactants and products at the molecular scale is proposed in Fig.2.

#### - Pechini method (Pech), Figs. 1(a) and 2(a)

30 years ago, Pechini [24] proposed a method to synthesize pure oxides based on the ability of  $\alpha$ -hydroxy acids, such as citric acid, to form chelates (citric acid-metal) with different cations (Fig. 2(a)). The cation precursors (nitrates and sulfates) and citric acid are dissolved in distilled water and then mixed with polyhydroxy alcohol, such as ethylene glycol [25]. By heating this mixture, water evaporates and polyesterification takes place, which leads to the formation of a

metal-polymer network (Fig. 2(a)). The major aim of this synthesis route is to achieve a random distribution of cations within the resin. The advantage is that the viscosity and the molecular mass of the polymer can be controlled by varying the resin content [26]. The resin content noted Rc is given by equation (1):

$$\%Rc = \frac{m_{\text{resin}}}{m_{\text{resin}} + m_{\text{oxide}}} \times 100 \quad (1)$$

where  $m_{\text{oxide}}$  is the mass of the final oxide to be produced (ye'elimite in the present case), calculated from the known masses of the precursors, and  $m_{\text{resin}}$  is the mass of the organic part. In the PECH method,  $m_{\text{resin}}$  is the mass of citric acid and ethylene glycol in the mixture. For the other two methods described and used in this study, namely the OSE and the SPC methods,  $m_{\text{resin}}$  corresponds respectively to the mass of polyvinyl alcohol and the mass of citric acid in the mixture.

The salts corresponding to a final mass of 2 g of ye'elimite were dissolved in 30 ml of deionized water. The resin was composed of 60 wt% of citric acid  $\text{HOC}(\text{CH}_2\text{CO}_2\text{H})_2\text{CO}_2\text{H}$  (N°CAS: 177-92-9, Fisher Scientific) and 40 wt% of ethylene glycol  $\text{HOCH}_2\text{CH}_2\text{OH}$  (N°CAS: 107-21-1, Fisher Scientific). Rc was fixed at 70% and 95%. The choice of Rc is based on work by Nettleship et al. [15]. The masses of each chemical reactant for Rc=70% and Rc=95% are presented in Table 2. The corresponding products are noted Pech70 and Pech95.

Citric acid was introduced according to the following sequence: dissolution in deionized water with a 1:3 molar ratio, addition to the solution of salts, mixing within a solution of ethylene glycol in order to promote polyesterification reactions. The mixture was then stirred at 80 °C for 8 h on a hot plate to evaporate water and to favor polymerization. The resulting viscous gel was completely dried at 150 °C for 2 h to become a crisp aerated gel (Fig. 1(a)). The crispy gel was calcined in a platinum crucible with a heating ramp of 5 °C min<sup>-1</sup>, up to a temperature

ranging between 400 °C and 1290 °C for 1 h. After cooling the furnace to room temperature, the samples were collected and stored in airtight plastic containers.

- **Organic steric entrapment method (OSE), Figs. 1(b) and 2(b)**

More recently, a new processing route has been developed. Unlike the Pechini-resin process, which involves chelation and polymerization, the OSE process consists of primarily steric entrapment of cations in the polymer network, namely Polyvinyl Alcohol (PVA). PVA ensures the homogenous distribution of the ions in its polymer network structure and prevents further agglomeration and/or precipitation from the solution (Fig. 2(b)) [9,10].

The starting salts were the same as for the Pechini process. The salts were dissolved in stoichiometric proportions in deionized water. Once the salts were completely dissolved, water containing 5 wt% of dissolved PVA (N°CAS: 9002-89-5, VWR Chemicals) was added. The molecular weight of PVA was 22000 g.mol<sup>-1</sup> with a degree of polymerization of 500 (monomers/polymer). The mass ratio of the PVA to cation sources was chosen in such a way that there were 4 times more positively charged valence ions from the cations than from the potentially charged –(OH) functional groups of the polymers [27]. In one PVA monomer, there is one hydroxyl –(OH) functional group. In the case of the 4:1 C<sub>4</sub>A<sub>3</sub> $\bar{S}$  cations to PVA hydroxyl ratio, the total positively charged valency of ions is 32 (4 Ca<sup>2+</sup> + 6 Al<sup>3+</sup> + 1 S<sup>6+</sup>). Thus 8 PVA monomers are used per 1 C<sub>4</sub>A<sub>3</sub> $\bar{S}$  molecule. The results of mass calculations are listed in Table 2.

After PVA addition to the initial mixture, water was evaporated by continuous stirring during heating at 80 °C on a hot plate. The resulting viscous gel was completely dried after several hours at 150 °C (Fig. 1(b)) and then thermally treated at different temperatures (400-1290 °C) in a muffle furnace with a heating rate of 5 °C min<sup>-1</sup>. After cooling the furnace to room temperature, the samples were stored in airtight plastic containers.

- **Self-propagating combustion synthesis (SPC), Figs. 1(c) and 2(c)**

Among the techniques of chemical synthesis, combustion synthesis is a novel route with a unique combination of the chemical sol–gel process and the combustion process. The success of the method is due to an intimate blending that is achieved among the constituents by using a suitable fuel or complexing agent, such as citric acid, in an aqueous media and an exothermic redox reaction between the fuel and an oxidizer (i.e. nitrates and sulfates) (Fig. 2(c)) [28]. The SPC method is characterized by the fact that once the initial exothermic reaction mixture is ignited by means of an external thermal source, a rapid (typically from 0.1 to 10 cm/s) high-temperature (1000-3000 °C) reaction wave propagates through the mixture in a self-sustained manner [29].

Combustion in a mixture of the salts with citric acid in an aqueous solution was carried out to synthesize a fine powder of ye'elimite. The citric acid was added to chelate  $\text{Ca}^{2+}$  and  $\text{Al}^{3+}$  in the solution (Fig. 2(c)) and as a suitable fuel for the combustion reaction. The molar ratio of citric acid to total moles of nitrate and sulfates ions was adjusted to 1:1 [30].

The aqueous solution was evaporated to a dry state by heating at 80 °C on a hot plate with continuous stirring. As the water evaporated, the solution became viscous and finally formed a very viscous gel (Fig. 1(c)). Increasing the temperature up to 150 °C led to the ignition of the gel. The reaction was initiated locally and the dried gel burnt in a self-propagating combustion manner until all of it was completely burnt out to form a loose powder (Fig. 1(c)) [31]. Finally, the as-burnt powders were calcined in air at different temperatures 400-1290 °C for 1 h with a heating rate of 5 °C min<sup>-1</sup>.

A comparison between the major steps of the three used chemical routes for ye'elimite synthesis at low temperature is given in Table 3. In the following, the term 'dried gel' will refer to the gels treated at 150 °C as explained in these three protocols. It should be kept in mind that during



this step, the gel prepared by the SPC method could be exposed in some points to a temperature higher than 150 °C [24].

## 2-2- Characterization techniques

The Differential Thermal Analysis (DTA) and the Thermogravimetric Analysis (TGA) of the dried gel was carried out using a Setaram SETSYS 24 apparatus. 15 mg of the sample was introduced into a platinum crucible and analyzed with a heating ramp of 20 °C min<sup>-1</sup> between 30 to 1100 °C. Previously calcined  $\alpha$ -Al<sub>2</sub>O<sub>3</sub> was used as a reference.

X-Ray Diffraction (XRD) data were collected at room temperature in the Bragg-Brentano geometry using a Bruker D8 Advance X-ray diffractometer with CuK $\alpha$  radiation ( $\lambda_{\text{Cu}} = 1.54056 \text{ \AA}$ , without monochromator; operating voltage of 40 kV and electric current 40 mA). The step scan was 0.02° with a time counting per step of 0.45 seconds. The sample was rotated during data collection at 15 rpm in order to increase particle statistics. The diffractometer was equipped with an energy-dispersive LYNXEYE XE-T detector for filtration of fluorescence and K $\beta$  radiation. Mineral phases of the synthesized samples were quantified by using the Rietveld method as implemented in the TOPAS 4.2 software. The fitting parameters were the background coefficients, the phase scales, the zero-shift error, the cell parameters, and the phase shape parameters. The peak shapes were fitted by using the pseudo-Voigt function. The Rietveld refinement strategy and the criteria for the selection of the best crystal structure data were based on the recent methods concerning diffraction and crystallography applied to anhydrous cements published by De la Torre et al. [32]. The structures used for fitting the crystalline phases and the respective ICSD (Inorganic Crystal Structure Database) codes are given in Table 4.

The broadening of the highest intensity peak, namely from the (202) planes ( $2\theta=23.6^\circ$ ), was used to determine the ye'elimite average crystallite size ( $D_{\text{crystallite}}$ ) using Scherrer's equation (2) [40]:

$$D_{\text{crystallite}} = \frac{0.89 \times \lambda}{\text{FWHM} \times \cos \theta} \quad (2)$$

$\lambda$  is the X-ray wavelength (0.15406 nm),  $\theta$  is the corresponding Bragg angle, FWHM is the Full Width at Half Maximum of the diffraction peak after subtraction of instrumental broadening. The instrumental broadening was determined using  $\text{LaB}_6$  as a reference (NIST standard reference material).

Powder morphology was examined by LEO 1530 VP field emission scanning electron microscopy (SEM) equipped with an EDS detector (Oxford INCA 250). The microscope was operated at a 1 kV accelerating voltage. This low voltage is necessary in order to avoid spoiling the sample. SEM samples were prepared by dispersing the powder in absolute ethanol. One drop of the suspension was then deposited on an aluminum support and dried in air. The specimens are stored in desiccators with silica gel prior to and after examination to prevent hydration or carbonation. The SEM observations were carried out without using a deposited conducting layer.

The particle size distribution of the synthesized ye'elimite powders was examined by two techniques which gave information at nanometric and micrometric scales, respectively. The first technique (nanometric scale) was image analysis (PSD-IA) of the SEM micrographs using ImageJ V1.51 software. A statistical analysis of the data was made using OriginPro V9.2 software. The particle size,  $D_{\text{particle}}$ , corresponds to the mean Feret maximum diameter estimated from a total of 160 ye'elimite particles ( $N_{\text{total}} = 160$ ). The standard deviation,  $\sigma$ , is estimated for each analyzed image.

The mean particle diameter of the distribution  $D_{\text{particle}}$  is calculated as follows:

$$D_{\text{Particle}} = \frac{1}{160} \sum_{i=1}^{160} D_F \quad (3)$$

where  $D_F$  refers to the maximum Feret diameter which can be defined as the distance between the most distant points on the projection of the particle (Fig. 3). Lastly, the standard deviation of the particle size distribution is calculated:

$$\sigma = \sqrt{\frac{1}{160-1} \sum_{i=1}^{160} (D_F - D_{\text{Particle}})^2} \quad (4)$$

The second technique (micrometric scale) was the laser size analysis (LSA) with a Mastersizer 2000 laser (Malvern). Prior to this measurement, the powder (approximately 50 mg) was mixed in 40 ml of absolute ethanol and the suspension was agitated for 1 min with the help of a Vibracell 75041-Bioblock scientific ultrasonic apparatus in order to break the weakest agglomerates.

### 3. Results and discussion

#### 3-1- Thermal analysis of the gel precursor

The thermal events that occur when heating the dried gels are shown in Fig. 4. The thermal events can be divided into four stages according to the temperature ranges. The phenomena associated with each temperature range are summarized in Table 5.

During the first stage between 30 and 200 °C, Pech70, Pech95, OSE and SPC lose respectively around 1, 0.9, 0.3 and 1.6 wt%. The mass losses are combined with a small endothermic signal. These events are attributed to the loss of residual water which is weakly physisorbed in the dried gels. The second stage for dried gels prepared by Pech70 method (Fig. 4(a)), Pech95 method (Fig. 4(b)), and SPC method (Fig. 4(d)), is in the range 370-750 °C, 300-700 °C, and

400-750 °C, respectively. The thermal analysis curves reveal the decomposition (burning) of organic bearing compounds (between 2 to 8 wt% loss), with a clear exothermic effect. The exothermic peak is the biggest for the dried gel prepared by the Pech95 method (Fig. 4(b)). It could be due to the high resin content. The second stage for the dried gel prepared by the OSE method occurs between 400 and 650 °C (Fig. 4(c)). It corresponds to the partial dehydration of PVA and its transformation into polyene, as suggested by the endothermic event at 556.8 °C accompanied with 2.1 % mass loss [41–43].

The third stage is between 850-860 and 950 °C for the dried gels prepared by Pech70, Pech95 and OSE method. In this temperature range, DTA curves show a small exothermic peak around 920.1 °C, 875.4 °C and 940.6 °C, respectively, with no significant mass loss. It could be related to a crystallization process and may indicate the possible formation of the  $C_4A_3\bar{S}$  phase. In the case of the dried gel prepared by the SPC method, the temperature range of stage III is between 750 and 855 °C (Fig. 4(d)). The exothermic peak at 800 °C with about 0.4 wt% loss is due to combustion of residual carbon [19].

Lastly, stage IV is between 900 and 1000 °C for the dried gels prepared by the SPC method, whereas it is from 940-950 to 1000 °C for the other dried gels. For dried gel prepared by OSE, a small exothermic peak appeared at 971.2 °C with no mass loss which could be attributed to ye'elimite crystal formation. For the other three dried gels, the exothermic peaks accompanied with small mass losses (0.1 to 1 wt%), are probably due to residual organic matter decomposition.

The main conclusions from the thermal analysis are the following: (i) the decomposition of organic products occurs mostly below 700 – 750°C, (ii) the crystallization of ye'elimite could start in the range 900 °C to 1000 °C.

### 3-2- Effect of calcination temperature on ye'elimite phase formation

Fig. 5 shows the XRD patterns of the four synthesized gels calcined at different temperatures in the range of 400 – 1290 °C. When the initial dried gels are calcined at 400 °C, the X-ray pattern presents a wide dome at low angles, indicating that amorphous phases are still present, and also crystalline peaks belonging to bassanite, anhydrite and calcium carbonate (Table 4). The presence of  $\overline{CC}$  could be explained by the presence of  $CO_2$  generated from the combustion reaction of organic precursors. As the calcination temperature increases to 1000 °C, the Grossite,  $CA_2$ , peak (noted G on Fig. 5) increases to a maximum, and then above this temperature decreases to a trace amount. Krotite, CA, (noted K on Fig. 5) peaks appear at 900 °C with an intensity that can be low (Figs. 5a and 5b) to very low (Fig. 5c) as the temperature increases. Concomitantly, ye'elimite ( $C_4A_3\overline{S}$ ) first appears at 900 °C and its peak intensity increases as the CA and  $CA_2$  peaks decrease in intensity. As the calcination temperature increases to 1250 °C, the corresponding diffraction pattern peak intensities of  $C_4A_3\overline{S}$  are significantly increased, which indicates a good crystallinity of the ye'elimite powders. At 1250 °C, all the diffraction peaks of the synthesized  $C_4A_3\overline{S}$  are attributed to the pure orthorhombic crystal phase of ye'elimite with a space group of Pcc2 and are in good agreement with the available standard ICSD#80361 [33]. By increasing the calcination temperature to 1290 °C, peaks related to CA can be slightly enhanced due to the decomposition of ye'elimite [2,44]. Thus, we confirm that 1250 °C is an optimum temperature for pure phase formation of the ye'elimite synthesized by chemical routes.

The purity of ye'elimite powders, synthesized by the Pech70, Pech95, OSE and SPC methods and calcined between 1000 and 1290 °C for 1 h, are presented in Table 6. To check the quality of the analysis fitting, the Rwp values are given in Table 6. The Rwp values are of the same order of magnitude as values found in literature [6,45]. The highest purity is obtained after calcination at 1250 °C for 1 h. The powder prepared by the OSE and SPC methods exhibit a

high purity of ye'elimite (about 98 wt%), whereas powders prepared by the Pech70 and Pech95 methods show ye'elimite purity of 79.4 wt% and 95.8 wt%, respectively. The differences on ye'elimite purity between the four methods could be explained by several factors such as the polymerization reaction, the changing viscosity of the precursor solution during the reaction and the chelation ability of the complexing agent. In our case, the formation of a polyester (reaction between citric acid and ethylene glycol) during the Pechini process is less beneficial for obtaining pure ye'elimite than when there is only one alcohol (PVA in the OSE route) or one acid (citric acid in the SPC route). Other parameters could play a role in the purity of the final powder. The influence of the polymer-to-cation ratio on the polymerization reaction was well discussed by Petrykin et Kakihana [46]. It was also noted in previous work that the amount of polymer and its molecular length could affect the distribution of the cations and hence the purity of the product [10,27,47].

### 3-3- Effect of calcination temperature on crystallite size of the synthesized ye'elimite

Fig. 7 presents the effect of calcination temperature on the crystallite size (calculated using Scherrer's equation (2)) of ye'elimite synthesized by the different chemical routes. The crystallite size increases with the calcination temperature, especially in the range from 1200 to 1250 °C. At 1250 °C, temperature at which the highest percentage of pure ye'elimite is obtained (Fig. 6), the crystallite size,  $D_{\text{crystallite}}$ , of powders prepared by the Pech70, Pech95, OSE and SPC methods are 50.2 nm, 53.6 nm, 57.5 nm and 50.9 nm, respectively. According to Quinelato et al. [42], increasing the distance between chelated cations leads to weak interactions among primary particles during crystallization, which yields small particles.

### 3-4- Microstructural characterization of ye'elimite synthesized at 1250 °C

By referring to XRD diffractograms (Fig. 5) and Rietveld quantitative Rietveld analysis (Table 6 and Fig. 6), we noted that the maximum of ye'elimite was obtained at 1250 °C. Consequently microstructural characterization has been carried out only for samples treated at 1250 °C.

Heat treatment at 1250 °C for 1 h shows the presence of nanometric particles that can form large agglomerates (Fig. 8). It could be the signature of the beginning of sintering of ye'elimite crystallites at 1250 °C.  $D_{\text{particle}}$ , determined by PSD-IA as explained in the experimental section, are 157 nm, 175 nm, 166 nm and 136 nm, respectively for the Pech70, Pech95, OSE and SPC methods (Fig. 8). A standard deviation,  $\sigma$ , of 146 nm was obtained using PVA (poly vinyl alcohol) as polymer agent for organic steric entrapment. A relatively narrow size distribution was observed for particles prepared by SPC ( $\sigma = 48$  nm), Pech70 ( $\sigma = 61$  nm) and Pech95 ( $\sigma = 65$  nm). These distributions are dependent on the amount and the nature of the organic part and hence are probably dependent on the amount of heat generated by the combustion reaction, which is a function of the starting resin [31]. Raab and Pöllmann [8] reported that the type and amount of the polymer govern its decomposition and influences the phase formation and the particle size of the synthesized product.

To conclude, the chemical routes permit to synthesize crystalline ye'elimite at 1250 °C instead of 1300 °C for the powder prepared by solid state synthesis [2–7]. Data at the nanometer scale show that the particles (around 136 – 175 nm) are about 3 times larger than the crystallites (51 to 57 nm). It could be the signature of the beginning of sintering of ye'elimite crystallites at 1250 °C.

Laser size analysis (volume % curves) of ye'elimite powder prepared at 1250 °C by the Pech method, OSE method and SPC method is presented in Fig. 9. The samples prepared by Pech95 method, OSE method and SPC method have a bimodal grain size distribution, where the maximum vol.% of the first grain size population is between 20 and 30  $\mu\text{m}$ . The second grain size population represents some residual agglomerates whose size ranges between 300 and 800  $\mu\text{m}$  for the sample prepared by Pech95 method, between 100 and 400  $\mu\text{m}$  for the sample prepared by OSE method and between 200 and 700  $\mu\text{m}$  for the sample prepared by SPC method. The powder prepared by Pech70 is slightly coarser than the other three powders and it presents

a monomodal grain size distribution, where the maximum vol.% corresponds to a particle size of 39  $\mu\text{m}$ .

The particles form hard agglomerates (Fig. 8) whose size range between 1 to 100  $\mu\text{m}$  as shown by the LSA curves (Fig. 10). The distribution is typical of what is required for a Portland cement and usually obtained after grinding the clinker [48]. In the present case, it is interesting to point out that this distribution is obtained directly after the sintering of the powders prepared by a chemical route and without the necessity of a grinding step. Somehow, compared to a Portland cement, the lower sintering temperature (1250  $^{\circ}\text{C}$  instead of 1450  $^{\circ}\text{C}$ ) and the absence of grinding implies some energy savings in the manufacturing process.

#### 4. Conclusion

This main conclusions of this work illustrated in Fig. 11 are:

- Fairly pure and fine ye'elimite particles were successfully obtained at 1250  $^{\circ}\text{C}$  for 1 hour by means of three chemical routes: the Pechini-method (with resin content 95%), the self-propagating combustion synthesis method and the organic steric entrapment method. The ye'elimite purity is respectively equal to 95.8 wt%, 97.9 wt% and 98.3 wt%.
- The application of quantitative Rietveld analysis to X-ray diffraction data indicates that ye'elimite with high purity (close to 98 wt%) was achieved by the organic steric entrapment method and by the self-propagating combustion synthesis. The formation of a polyester (reaction between citric acid and ethylene glycol) during the Pechini process inhibits the yield of pure ye'elimite. It is not the case when there is only one alcohol (PVA in the OSE route) or one acid (citric acid in the SPC route) involved.



- Referring to X-ray diffraction results, CA and CA<sub>2</sub> are the only intermediate crystalline phases detected. Upon increasing the heat treatment temperature, the amount of CA and CA<sub>2</sub> decreased being gradually transformed into the C<sub>4</sub>A<sub>3</sub> $\bar{S}$  phase.
- After a heat treatment at 1250 °C for 1 h, the nanosized crystallites (51 to 57 nm) form particles about 3 times larger (average size, D<sub>particle</sub>, between 136 and 175 nm) which could result from the sintering of the crystallites.
- The particles form hard agglomerates whose size range between 1 to 100 μm as shown by the laser size analysis curves (Fig. 8). The distribution, which is typical of a ground Portland clinker or cement, is obtained directly after sintering and without the necessity of a grinding step.

Thus, the present work provide an original protocol, using chemical routes, to synthesis nano-size ye'elimite particles showing small crystallite sizes and high purity. Moreover, the synthesized ye'elimite powders have the particle size distribution of a clinker. This could be usefully exploited for studying the kinetics and thermodynamics of ye'elimite hydration. In order to contribute to the understanding of ye'elimite hydration (the main phase of CSA cements), a thorough and exhaustive study about the hydration of the synthesized ye'elimite powders constitutes the main perspective of the present work.

### Acknowledgments

The authors would like to thank the members of the Groupement d'Intérêt Scientifique (GIS) SulfoCim for their useful comments. SulfoCim is an association between Association Technique de l'Industrie des Liants Hydrauliques (ATILH, Paris, France) and five academic laboratories : Institut Jean Lamour (UMR CNRS 7198 – Université de Lorraine, Nancy, France), Laboratoire de Génie Civil et Génie Mécanique (EA 3913 , INSA de Rennes, Rennes, France), Laboratoire de Physico-chimie des Polymères et Milieux Dispersés – Sciences et

Ingénierie de la Matière Molle (UMR CNRS 7615 – UPMC – ESPCI, Paris, France),  
 Laboratoire des Solides Irradiés (UMR CNRS 7642 – CEA – Ecole Polytechnique, Palaiseau,  
 France), Science des Procédés Céramiques et de Traitements de Surface (UMR CNRS 7315 –  
 Université de Limoges, Limoges, France).

## References

- [1] E. Gartner, T. Sui, Alternative cement clinkers, *Cem. Concr. Res.* (2017). doi:10.1016/j.cemconres.2017.02.002.
- [2] Y. El Khessaimi, Y. El Hafiane, A. Smith, R. Trauchessec, C. Diliberto, A. Lecomte, Solid-state synthesis of pure ye'elimite, *J. Eur. Ceram. Soc.* (2018). doi:10.1016/j.jeurceramsoc.2018.03.018.
- [3] F. Winnefeld, S. Barlag, Calorimetric and thermogravimetric study on the influence of calcium sulfate on the hydration of ye'elimite, *J. Therm. Anal. Calorim.* 101 (2009) 949–957. doi:10.1007/s10973-009-0582-6.
- [4] A. Cuesta, A.G. De la Torre, E.R. Losilla, V.K. Peterson, P. Rejmak, A. Ayuela, C. Frontera, M.A. Aranda, Structure, atomistic simulations, and phase transition of stoichiometric yeelimite, *Chem. Mater.* 25 (2013) 1680–1687. doi: 10.1021/cm400129z.
- [5] A. Cuesta, A.G. De la Torre, E.R. Losilla, I. Santacruz, M.A. Aranda, Pseudocubic crystal structure and phase transition in doped ye'elimite, *Cryst. Growth Des.* 14 (2014) 5158–5163. doi: 10.1021/cg501290q.
- [6] A. Cuesta, G. Álvarez-Pinazo, S.G. Sanfélix, I. Peral, M.A. Aranda, A.G. De la Torre, Hydration mechanisms of two polymorphs of synthetic ye'elimite, *Cem. Concr. Res.* 63 (2014) 127–136. doi:10.1016/j.cemconres.2014.05.010.
- [7] F. Winnefeld, B. Lothenbach, Hydration of calcium sulfoaluminate cements-experimental findings and thermodynamic modelling, *Cem. Concr. Res.* 40 (2010) 1239–1247. doi: 10.1016/j.cemconres.2009.08.014.
- [8] B. Raab, H. Pöllmann, 3. Synthesis of highly reactive pure cement phases, in: H. Pöllmann (Ed.), *Cem. Mater., De Gruyter, Berlin, Boston*, 2017: pp. 61–102. doi:10.1515/9783110473728-004.
- [9] Song Jong-Taek, Young J. Francis, Direct Synthesis and Hydration of Calcium Aluminosulfate ( $\text{Ca}_4\text{Al}_6\text{O}_{16}\text{S}$ ), *J. Am. Ceram. Soc.* 85 (2004) 535–539. doi:10.1111/j.1151-2916.2002.tb00129.x.
- [10] S.-J. Lee, W.M. Kriven, Synthesis and hydration study of Portland cement components prepared by the organic steric entrapment method, *Mater. Struct.* 38 (2005) 87–92. doi:10.1617/14018.
- [11] B. Raab, H. Pöllmann, Synthesis of pure cement phases by different synthesis methods, in: *Calcium Aluminate Cements, Proceedings of the Centenary Conference*, Edited by C.H. Fentiman, T.J. Managbhai and K.L. Scrivener, 2008.
- [12] J.J. Thomas, S. Ghazizadeh, E. Masoero, Kinetic mechanisms and activation energies for hydration of standard and highly reactive forms of  $\beta$ -dicalcium silicate ( $\text{C}_2\text{S}$ ), *Cem. Concr. Res.* 100 (2017) 322–328. doi: 10.1016/j.cemconres.2017.06.001.
- [13] S.-H. Hong, J.F. Young, Hydration kinetics and phase stability of dicalcium silicate synthesized by the Pechini process, *J. Am. Ceram. Soc.* 82 (1999) 1681–1686. doi: 10.1111/j.1151-2916.1999.tb01986.x.

- [14] Y.-M. Kim, S.-H. Hong, Influence of minor ions on the stability and hydration rates of  $\beta$ -dicalcium silicate, *J. Am. Ceram. Soc.* 87 (2004) 900–905. doi: 10.1111/j.1551-2916.2004.00900.x.
- [15] I. Nettleship, J.L. Shull, W.M. Kriven, Chemical preparation and phase stability of  $\text{Ca}_2\text{SiO}_4$  and  $\text{Sr}_2\text{SiO}_4$  powders, *J. Eur. Ceram. Soc.* 11 (1993) 291–298. doi:10.1016/0955-2219(93)90028-P.
- [16] A. Zapata, P. Bosch, Low temperature preparation of belitic cement clinker, *J. Eur. Ceram. Soc.* 29 (2009) 1879–1885. doi: 10.1016/j.jeurceramsoc.2008.11.004.
- [17] D.A. Fumo, M.R. Morelli, A.M. Segadaes, Combustion synthesis of calcium aluminates, *Mater. Res. Bull.* 31 (1996) 1243–1255. doi: 10.1016/0025-5408(96)00112-2.
- [18] Tas A. Cüneyt, Chemical Preparation of the Binary Compounds in the Calcia-Alumina System by Self-Propagating Combustion Synthesis, *J. Am. Ceram. Soc.* 81 (2005) 2853–2863. doi:10.1111/j.1151-2916.1998.tb02706.x.
- [19] H.C. Yi, J.Y. Guigné, J.J. Moore, F.D. Schowengerdt, L.A. Robinson, A.R. Manerbino, Preparation of calcium aluminate matrix composites by combustion synthesis, *J. Mater. Sci.* 37 (2002) 4537–4543. doi:10.1023/A:1020671626797.
- [20] Z. He, W. Liang, L. Wang, J. Wang, Synthesis of  $\text{C}_3\text{S}$  by sol-gel technique and its features, *J. Wuhan Univ. Technol.-Mater Sci Ed.* 25 (2010) 138–141. doi:10.1007/s11595-010-1138-0.
- [21] Gülgün Mehmet A., Popoola Oludele O., Kriven Waltraud M., Chemical Synthesis and Characterization of Calcium Aluminate Powders, *J. Am. Ceram. Soc.* 77 (2005) 531–539. doi:10.1111/j.1151-2916.1994.tb07026.x.
- [22] J.W. Bullard, H.M. Jennings, R.A. Livingston, A. Nonat, G.W. Scherer, J.S. Schweitzer, K.L. Scrivener, J.J. Thomas, Mechanisms of cement hydration, *Cem. Concr. Res.* 41 (2011) 1208–1223. doi:10.1016/j.cemconres.2010.09.011.
- [23] M.M. Costoya Fernández, Effect of particle size on the hydration kinetics and microstructural development of tricalcium silicate, PhD thesis, EPFL Lausanne, Switzerland (2008). doi: 10.5075/epfl-thesis-4102.
- [24] M.P. Pechini, Method of preparing lead and alkaline earth titanates and niobates and coating method using the same to form a capacitor (1967). Patent number US3330697A.
- [25] T. Barbier, Synthesis and characterization of new materials with colossal permittivity, PhD Thesis, Tours, France (2012).
- [26] X. Li, V. Agarwal, M. Liu, W.S. Rees, Investigation of the mechanism of sol-gel formation in the  $\text{Sr}(\text{NO}_3)_2$ /citric acid/ethylene glycol system by solution state  $^{87}\text{Sr}$  nuclear magnetic resonance spectroscopy, *J. Mater. Res.* 15 (2000) 2393–2399. doi: 10.1557/JMR.2000.0344.
- [27] S.J. Lee, E.A. Benson, W.M. Kriven, Preparation of Portland cement components by poly (vinyl alcohol) solution polymerization, *J. Am. Ceram. Soc.* 82 (8) (1999) 2049–2055. doi: 10.1111/j.1151-2916.1999.tb02039.x.
- [28] K.H. Wu, T.H. Ting, M.C. Li, W.D. Ho, Sol-gel auto-combustion synthesis of  $\text{SiO}_2$ -doped  $\text{NiZn}$  ferrite by using various fuels, *J. Magn. Magn. Mater.* 298 (1) (2006) 25–32. doi: 10.1016/j.jmmm.2005.03.008.
- [29] A.S. Mukasyan, P. Epstein, P. Dinka, Solution combustion synthesis of nanomaterials, *Proc. Combust. Inst.* 31 (2) (2007) 1789–1795. doi:10.1016/j.proci.2006.07.052.
- [30] J.C. Restrepo, A. Chavarriaga, O.J. Restrepo, J.I. Tobón, Synthesis of Hydraulically Active Calcium Silicates Produced by Combustion Methods, *MRS Online Proc. Libr. Arch.* 1768 (2015). doi:10.1557/opl.2015.321.
- [31] A.S. Rogachev, A.S. Mukasyan, Combustion for Material Synthesis, CRC Press, Taylor and Francis Group (2014). ISBN 9781482239515.

- [32] Á.G. De la Torre, I. Santacruz, L. León-Reina, A. Cuesta, M.A.G. Aranda, 1. Diffraction and crystallography applied to anhydrous cements, in: H. Pöllmann (Ed.), *Cem. Mater.*, De Gruyter, Berlin, Boston, 2017: pp. 3–30. doi:10.1515/9783110473728-002.
- [33] N.J. Calos, C.H.L. Kennard, A.K. Whittaker, R.L. Davis, Structure of calcium aluminate sulfate  $\text{Ca}_4\text{Al}_6\text{O}_{16}\text{S}$ , *J. Solid State Chem.* 119 (1995) 1–7. doi:10.1016/0022-4596(95)80002-7.
- [34] W. Hörkner, H. Müller-Buschbaum, Zur kristallstruktur von  $\text{CaAl}_2\text{O}_4$ , *J. Inorg. Nucl. Chem.* 38 (1976) 983–984. doi:10.1016/0022-1902(76)80011-5.
- [35] V.I. Ponomarev, D.M. Kheiker, N.V. Belov, Crystal structure of calcium dialuminate,  $\text{CA}_2$ , *Sov. Phys. Crystallogr. USSR.* 15 (1971) 995–+.
- [36] D. Grier, G. McCarthy, North Dakota State University, Fargo, North Dakota, USA, ICDD Grant-in-Aid 1991, Powder Diffr. File Int. Cent. Diffr. Data. (1994).
- [37] E.N. Maslen, V.A. Streltsov, N.R. Streltsova, X-ray study of the electron density in calcite,  $\text{CaCO}_3$ , *Acta Crystallogr. B.* 49 (1993) 636–641. doi: 10.1107/S0108768193002575.
- [38] G.C.H. Cheng, J. Zussman, The crystal structure of anhydrite ( $\text{CaSO}_4$ ), *Acta Crystallogr.* 16 (1963) 767–769. doi: 10.1107/S0365110X63001997.
- [39] C. Bezou, A. Nonat, J.C. Mutin, A.N. Christensen, M.S. Lehmann, Investigation of the crystal structure of  $\gamma\text{-CaSO}_4$ ,  $\text{CaSO}_4 \cdot 0.5\text{H}_2\text{O}$ , and  $\text{CaSO}_4 \cdot 0.6\text{H}_2\text{O}$  by powder diffraction methods, *J. Solid State Chem.* 117 (1) (1995) 165–176. doi: 10.1006/jssc.1995.1260.
- [40] A.W. Burton, K. Ong, T. Rea, I.Y. Chan, On the estimation of average crystallite size of zeolites from the Scherrer equation: a critical evaluation of its application to zeolites with one-dimensional pore systems, *Microporous Mesoporous Mater.* 117 (1-2) (2009) 75–90. doi: 10.1016/j.micromeso.2008.06.010.
- [41] J.W. Gilman, D.L. VanderHart, T. Kashiwagi, Thermal Decomposition Chemistry of Poly (vinyl alcohol) Char Characterization and Reactions with Bismaleimides, in: *Fire and Polymers II*, Ed. G. L. Nelson, American Chemical Society Publications (1995) Chapter 11, pp 161–185. doi: 10.1021/bk-1995-0599.ch011.
- [42] M. Wiśniewska, S. Chibowski, T. Urban, D. Sternik, Investigation of the alumina properties with adsorbed polyvinyl alcohol, *J. Therm. Anal. Calorim.* 103 (1) (2011) 329–337. doi: 10.1007/s10973-010-1040-1.
- [43] P. Budrugaec, Kinetics of the complex process of thermo-oxidative degradation of poly (vinyl alcohol), *J. Therm. Anal. Calorim.* 92 (1) (2008) 291–296. doi: 10.1007/s10973-007-8770-8.
- [44] F. Puertas, M.B. Varela, S.G. Molina, Kinetics of the thermal decomposition of  $\text{C}_4\text{A}_3\text{S}$  in air, *Cem. Concr. Res.* 25 (1995) 572–580. doi:10.1016/0008-8846(95)00046-F.
- [45] X. Li, Y. Zhang, X. Shen, Q. Wang, Z. Pan, Kinetics of calcium sulfoaluminate formation from tricalcium aluminate, calcium sulfate and calcium oxide, *Cem. Concr. Res.* 55 (2014) 79–87. doi: 10.1016/j.cemconres.2013.10.006.
- [46] V. Petrykin, M. Kakihana, Chemistry and applications of polymeric gel precursors, In: Klein L., Aparicio M., Jitianu A. (eds) *Handbook of Sol-Gel Science and Technology*. Springer, Cham, (2018) 81–112. doi: 10.1007/978-3-319-32101-14.
- [47] M.H. Nguyen, S.J. Lee, W.M. Kriven, Synthesis of oxide powders by way of a polymeric steric entrapment precursor route, *J. Mater. Res.* 14 (8) (1999) 3417–3426. doi:10.1557/JMR.1999.0462.
- [48] H.F.W. Taylor, *Cement chemistry*, 2<sup>nd</sup> edition, edited by Thomas Telford, London, 1997.

## Figure captions

Figure 1	Flow diagram showing the processing routes used in the present work: Pechini (Rc=70%) Pech70 or (Rc=95%) Pech95 (a), Organic steric entrapment method OSE (b) and Self-propagating combustion SPC (c). Rc represents the resin content calculated from equation 1.
Figure 2-a	Proposed chemical reactions describing the polymeric process of the Pechini method. The gray spheres represent carbon atoms and the yellow spheres represent sulfur atoms, whereas white, red, pink, purple and green spheres identify hydrogen, oxygen, nitrogen, aluminum and calcium, respectively.
Figure 2-b	Proposed chemical reactions describing the polymeric process of the OSE method. The gray spheres represent carbon atoms and the yellow spheres represent sulfur atoms, whereas white, red, pink, purple and green spheres identify hydrogen, oxygen, nitrogen, aluminum and calcium, respectively.
Figure 2-c	Proposed chemical reactions describing the polymeric process of the SPC method. The gray spheres represent carbon atoms and the yellow spheres represent sulfur atoms, whereas white, red, pink, purple and green spheres identify hydrogen, oxygen, nitrogen, aluminum and calcium, respectively.
Figure 3	Maximum Feret diameter applied to a projection of a 3D schematic nano-particle.
Figure 4	DTA-TGA of gel precursor made by the Pech70 method (a), Pech95 method (b), OSE method (c) and SPC method (d).
Figure 5	XRD patterns of the gel precursor, synthesized by the Pech70 method (a), Pech95 method (b), OSE method (c) and SPC method (d), calcined at 400 °C, 700 °C, 900 °C, 1000°C, 1200 °C, 1250 °C and 1290 °C for 1 h (Y= Ye'elimite, G = Grossite, K = Krotite, C = CaO, B = Bassanite, Cc = Calcium carbonate, An = Anhydrite).
Figure 6	The Rietveld quantitative analysis plots of ye'elimite powder prepared at 1250 °C by the Pech70 method (a), Pech95 method (b), OSE method (c) and SPC method (d).
Figure 7	Effect of calcination temperature on the crystallite size (calculated from (2)) of ye'elimite synthesized by the different chemical routes.
Figure 8	SEM micrographs of the gels precursors calcined at 1250 °C for 1 h. Zooms show that each agglomerate consists of nanometric particles. Their average diameter, $D_{particle}$ , as well as the deviation, determined by PSD-IA, are presented.
Figure 9	Laser size analysis (volume % curves) of ye'elimite powder prepared at 1250 °C by the Pech method, OSE method and SPC method.
Figure 10	Laser size analysis (cumulative volume % curves) of ye'elimite powder prepared at 1250 °C by the Pech method, OSE method and SPC method.
Figure 11	Radar chart to summarize all the parameters of ye'elimite powder prepared at 1250 °C by the Pech method, OSE method and SPC method (values between brackets represent the maximum value of each parameter).

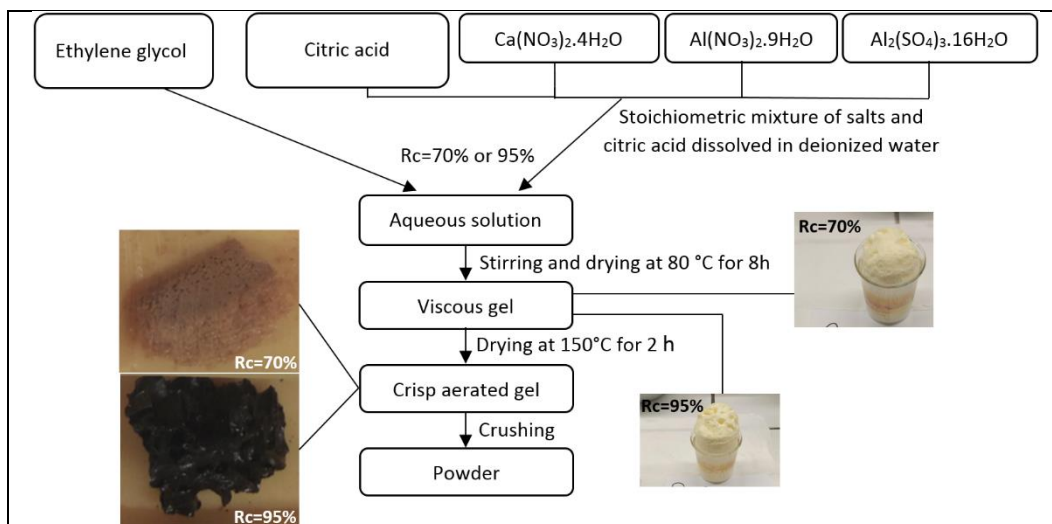


Figure 1-a

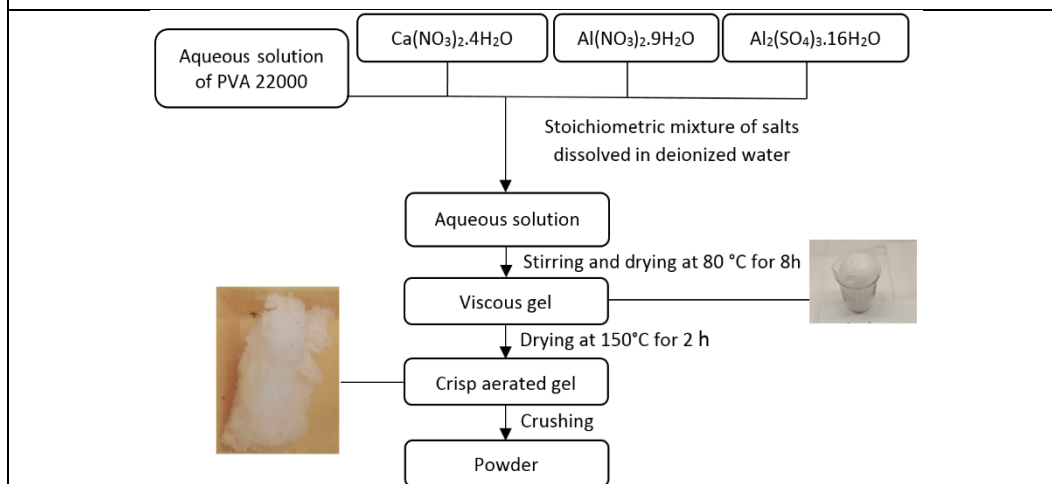


Figure 1-b

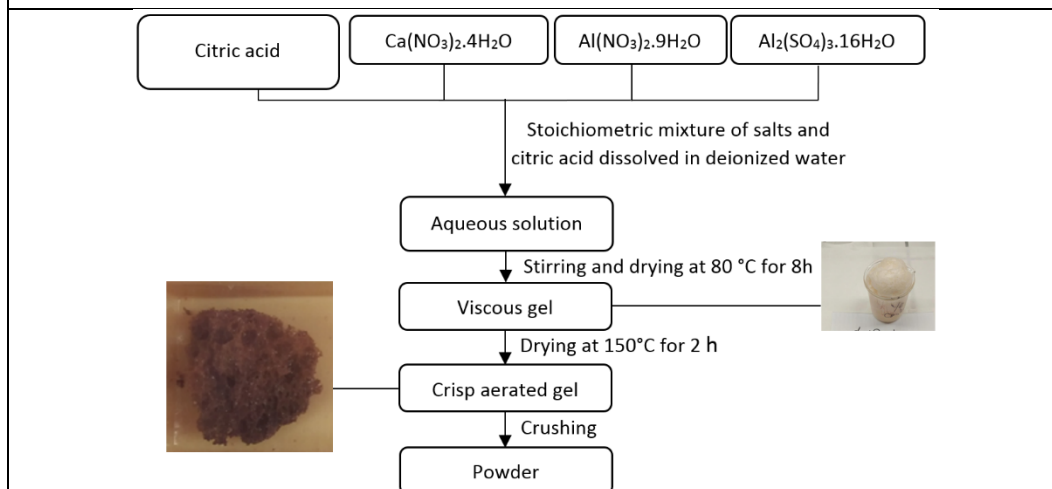


Figure 1-c

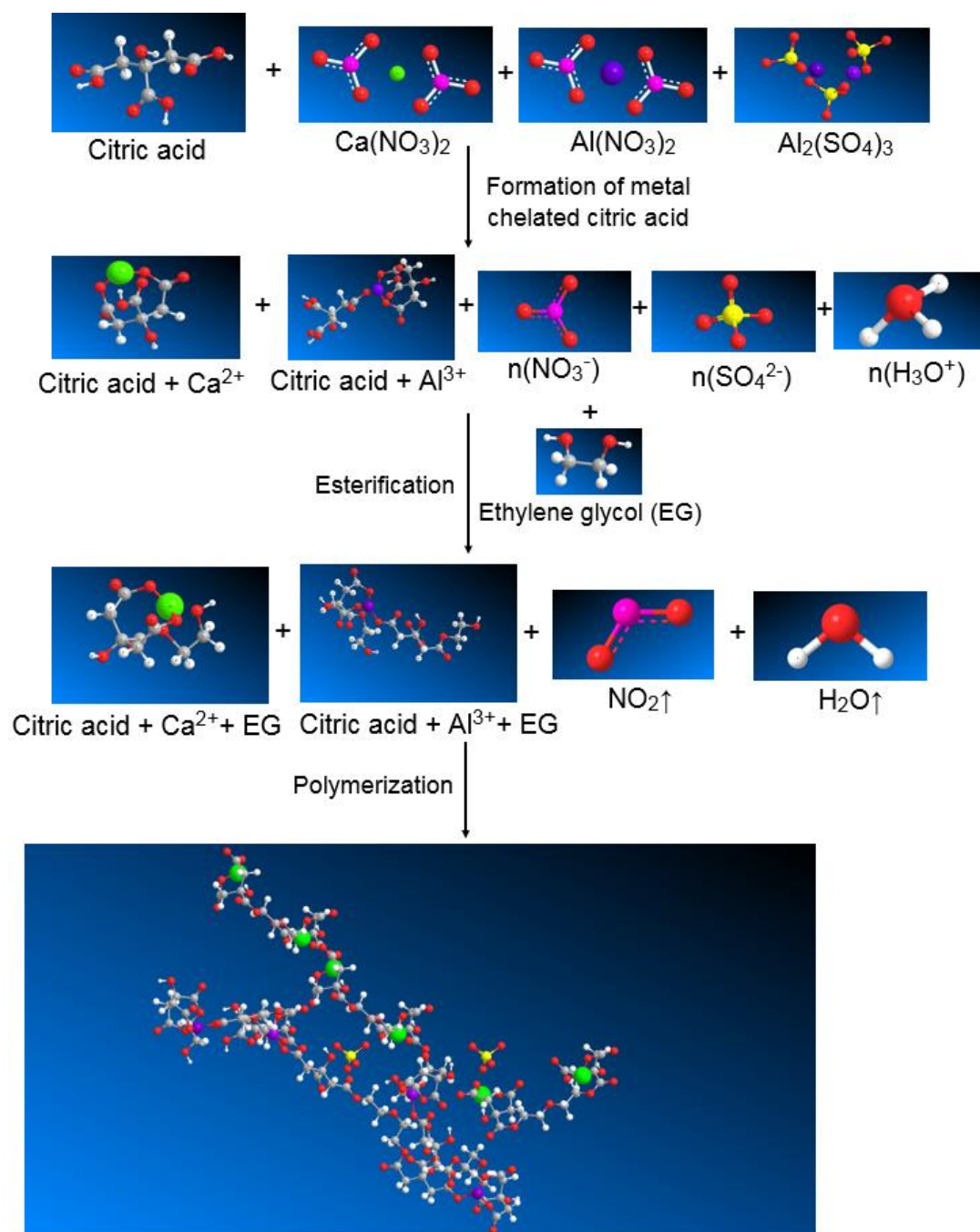


Figure 2-a

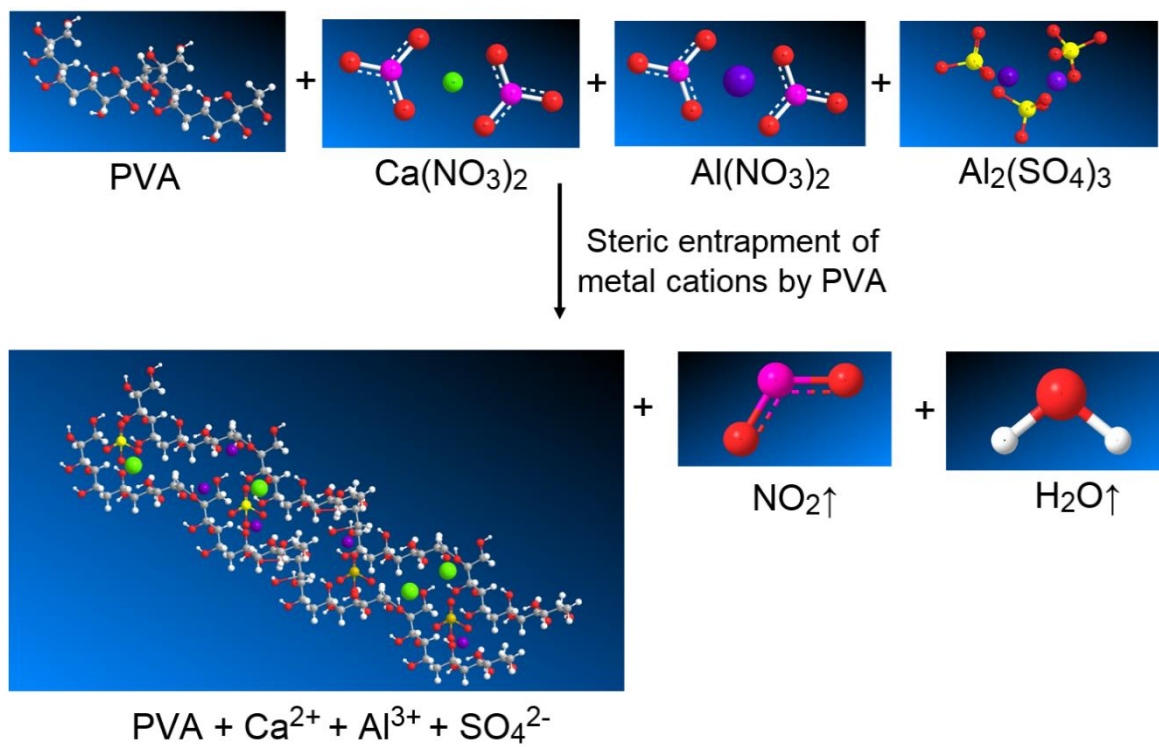


Figure 2-b



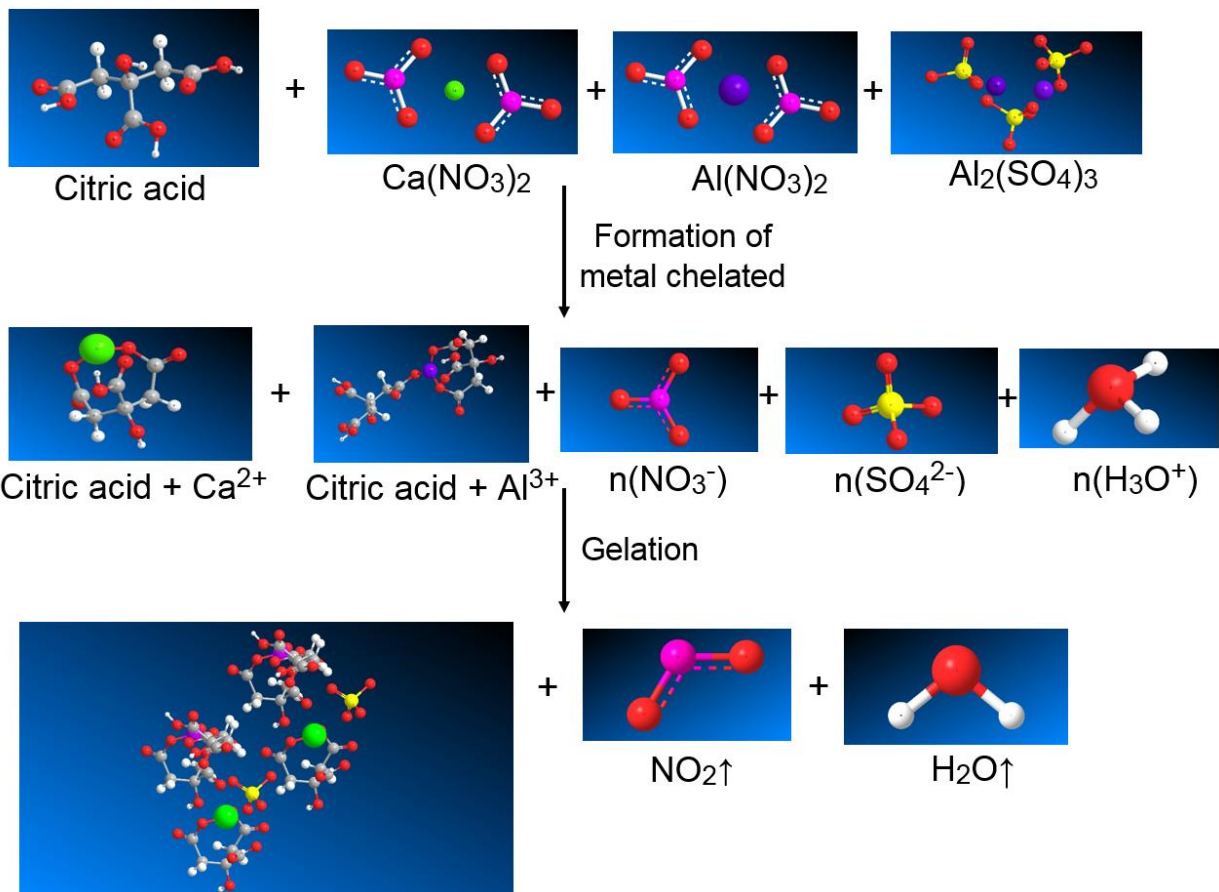


Figure 2-c

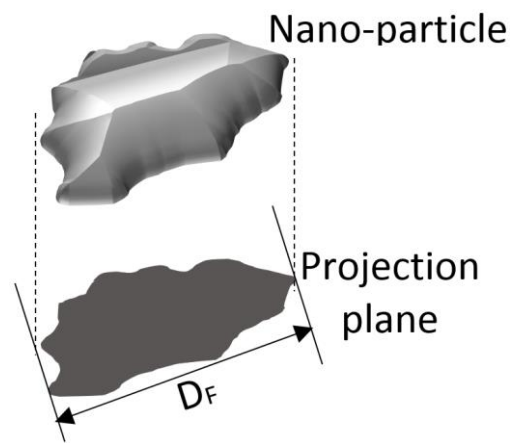


Figure 3

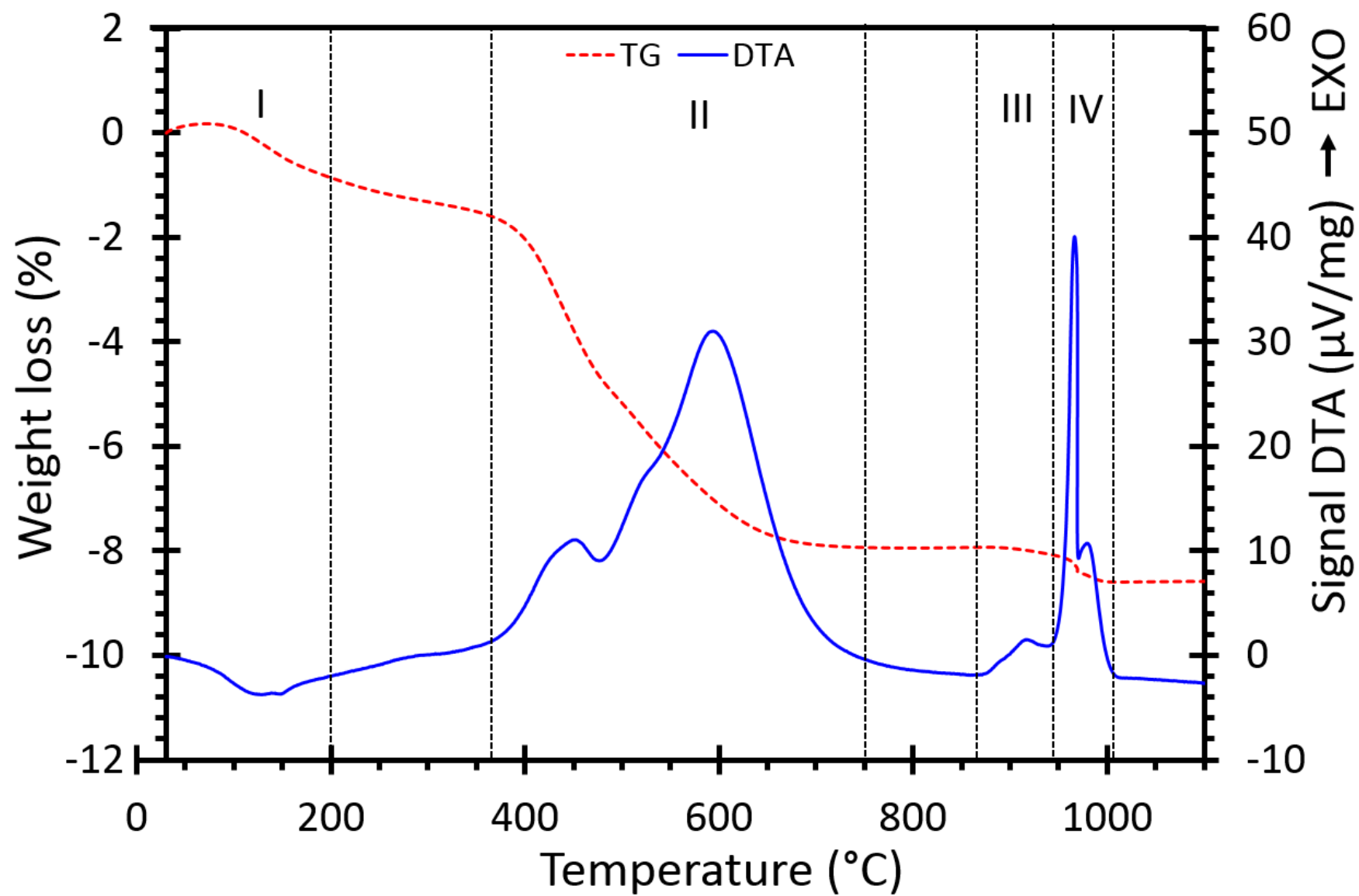


Figure 4-a

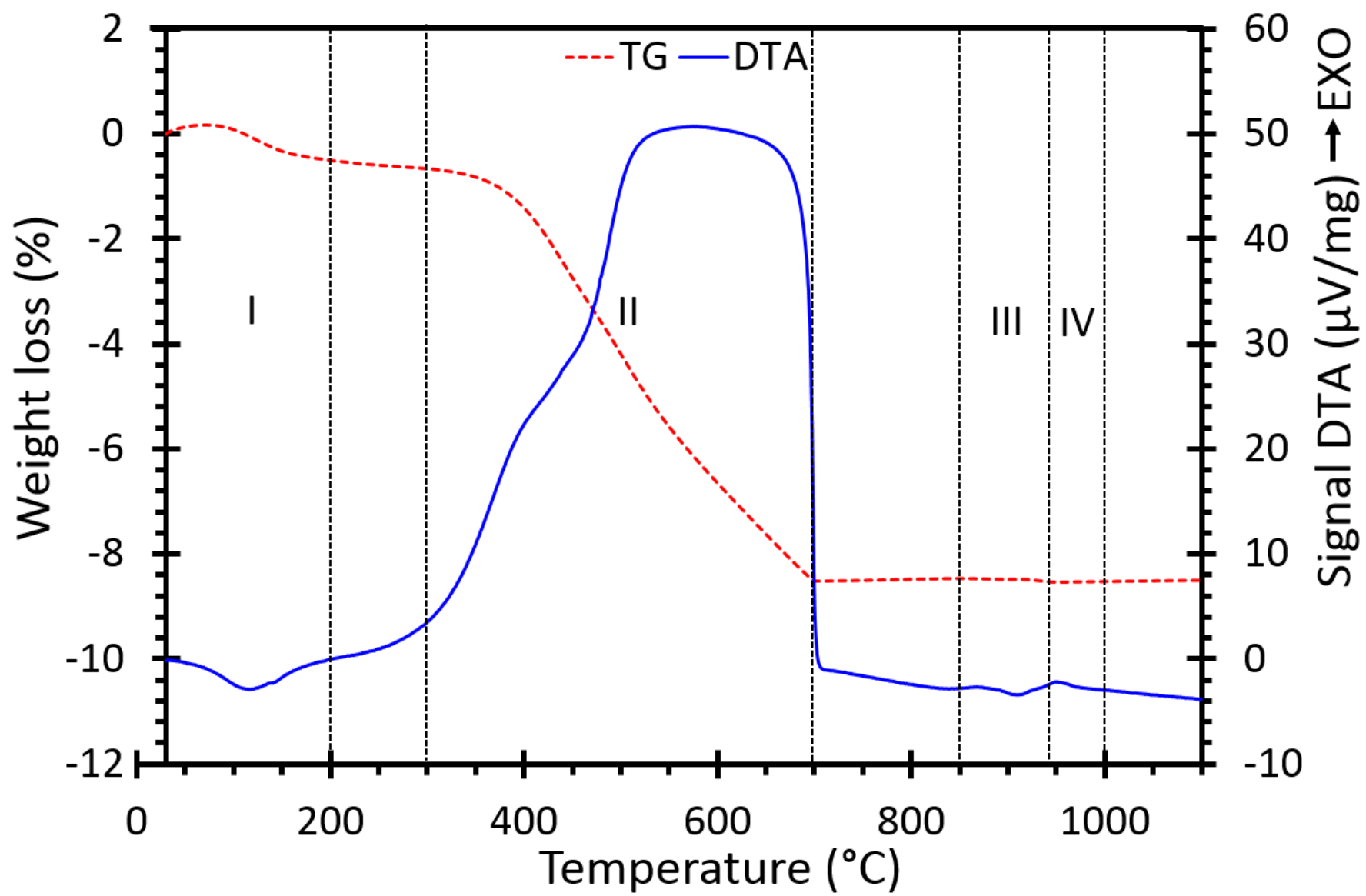


Figure 4-b

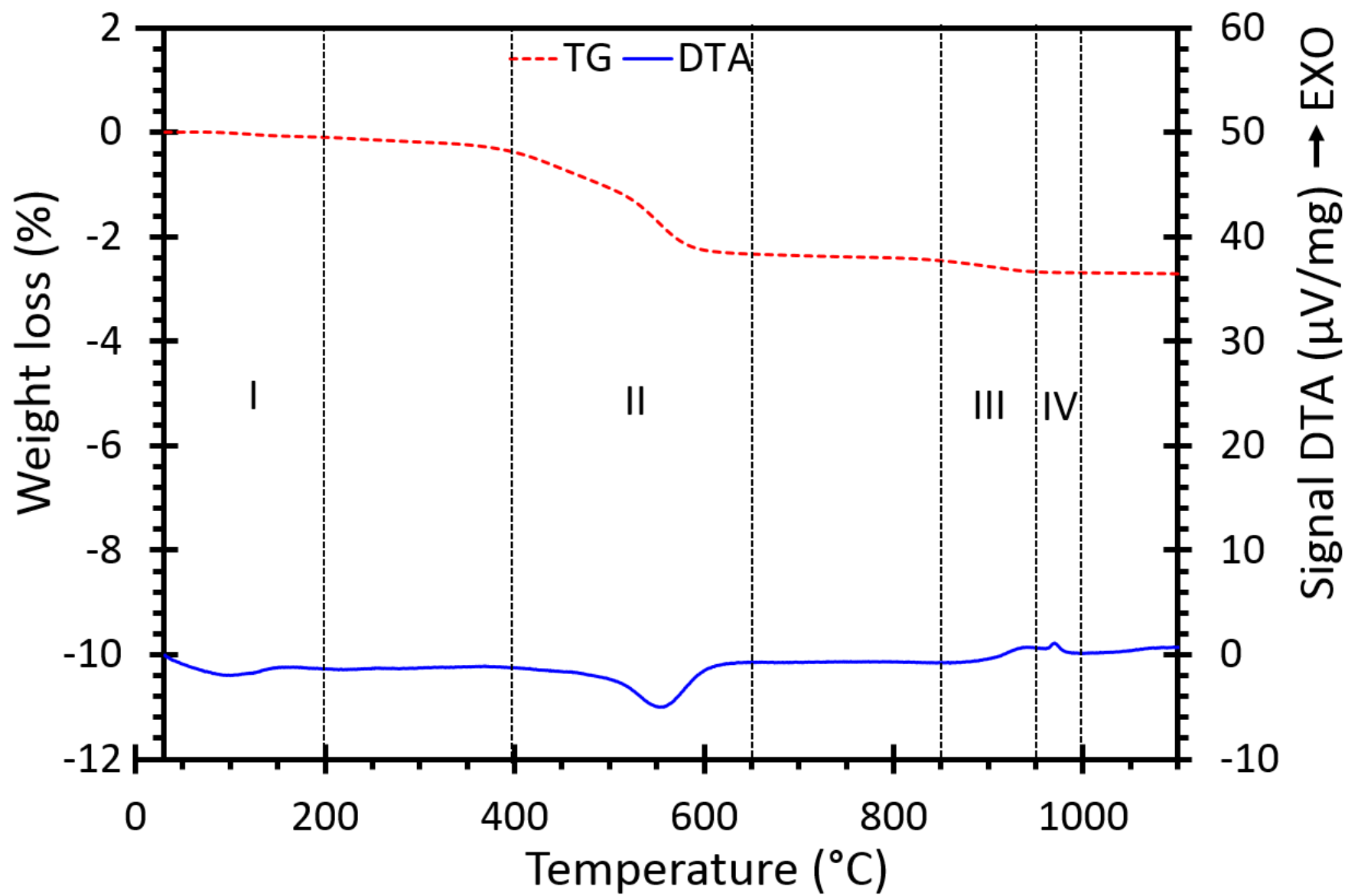


Figure 4-c

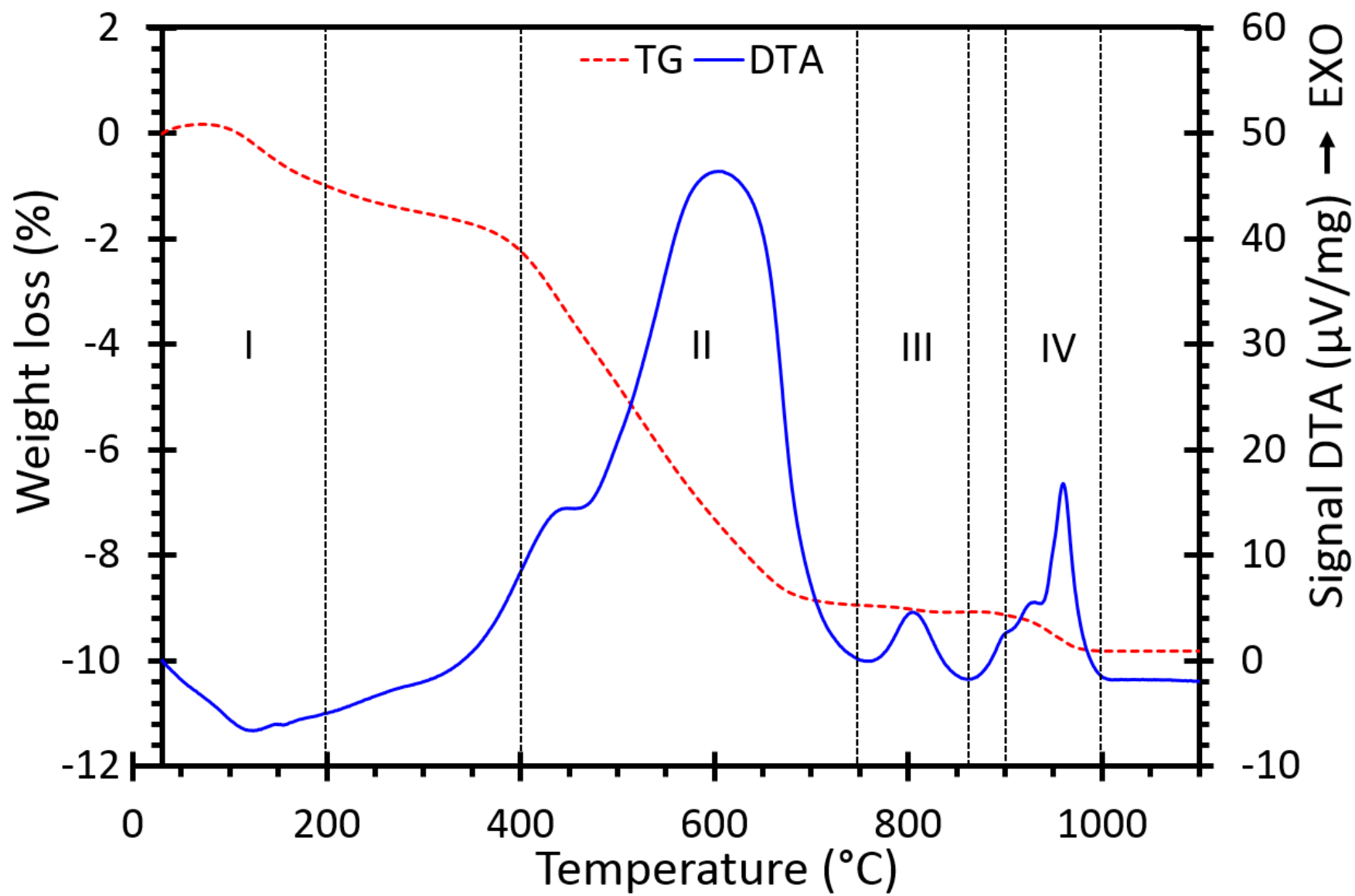


Figure 4-d

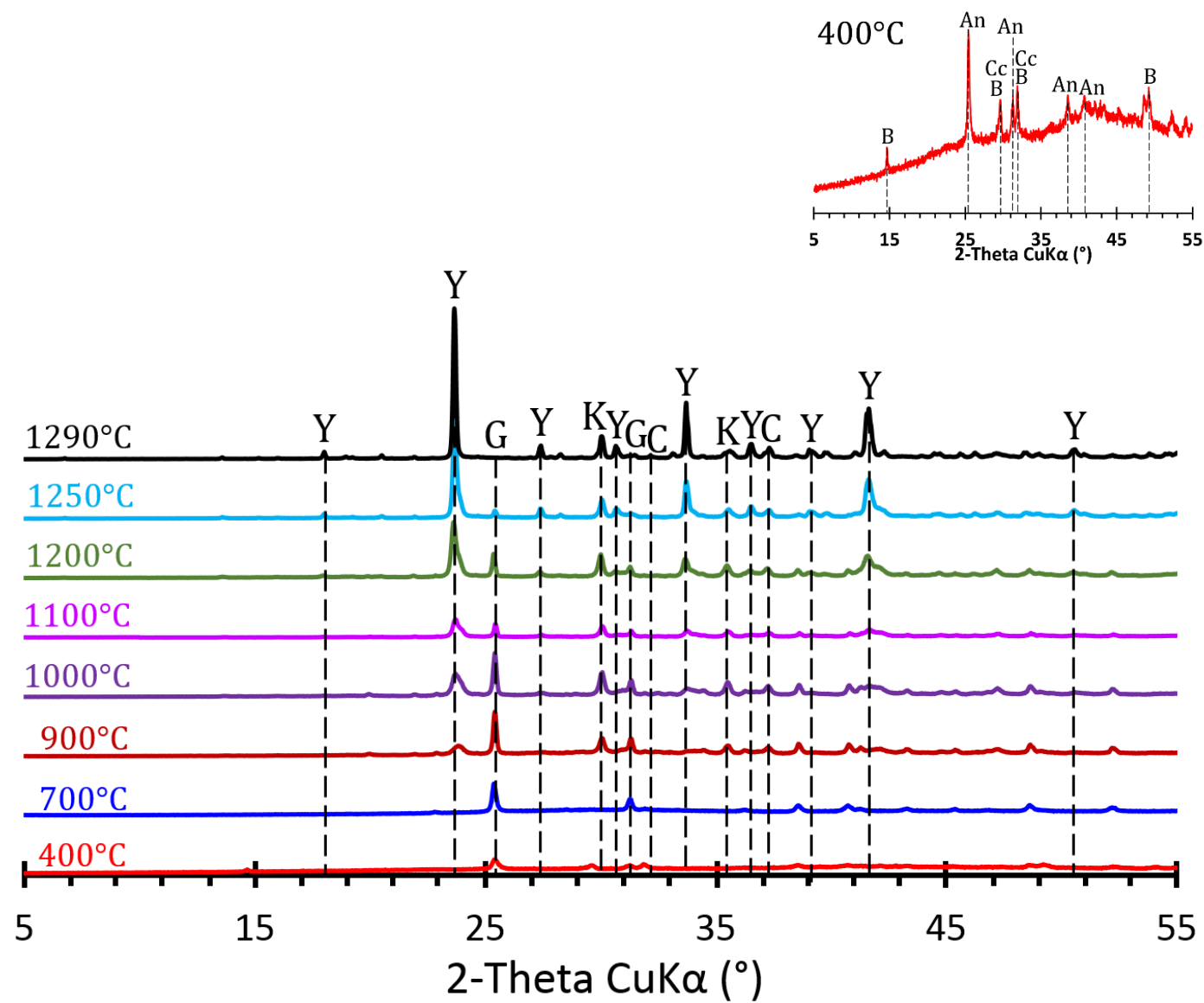


Figure 5-a

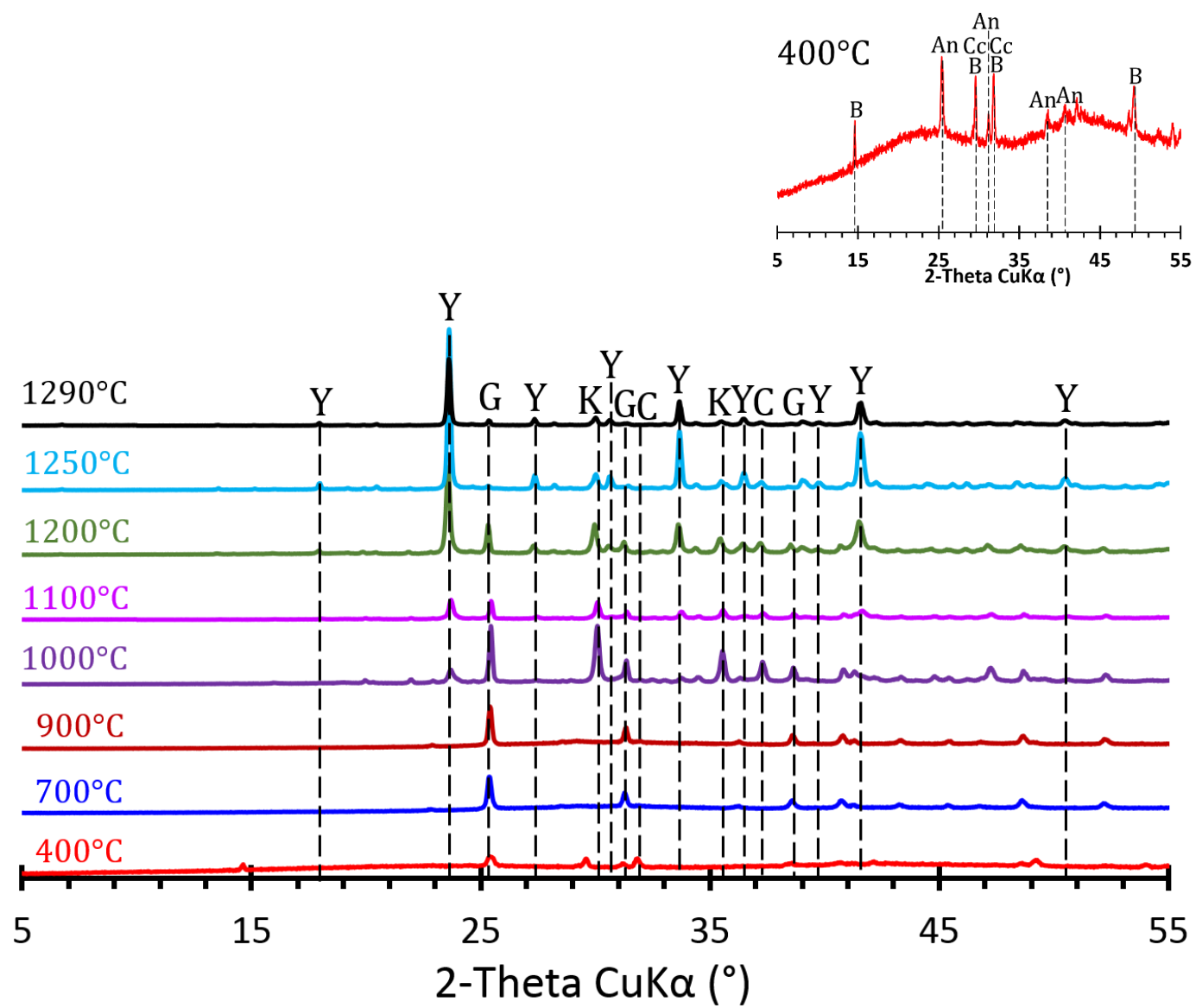


Figure 5-b



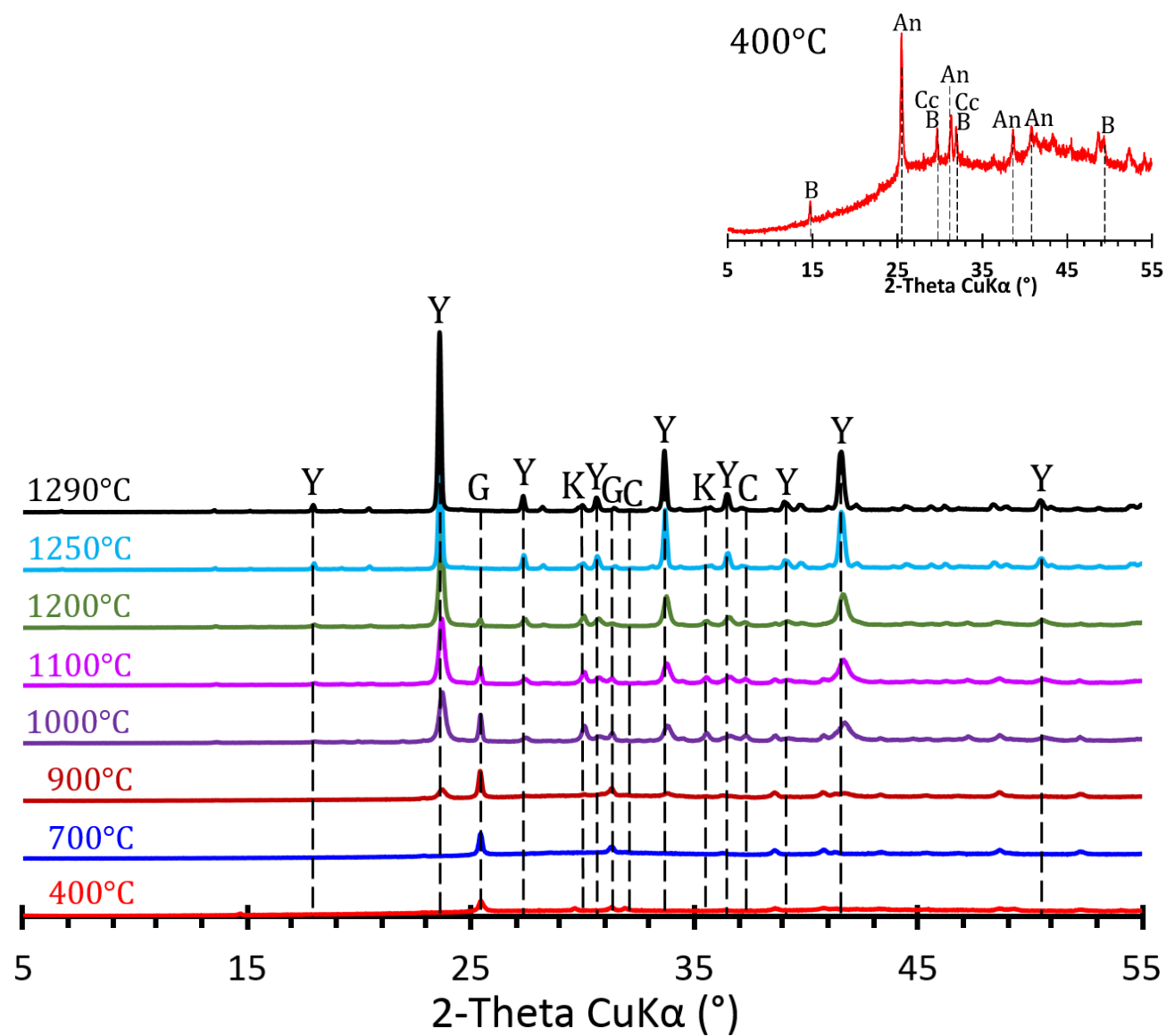


Figure 5-c

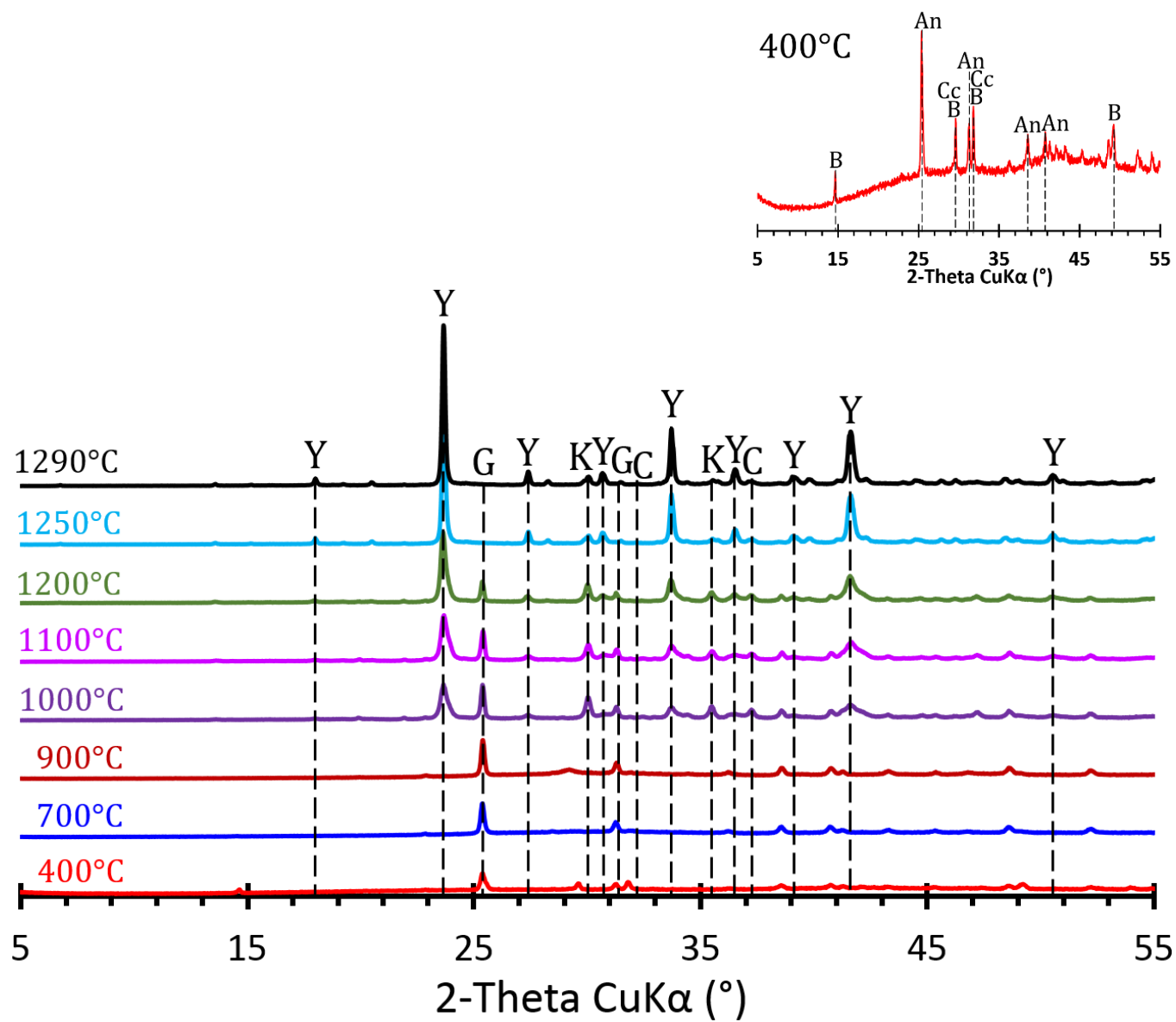


Figure 5-d

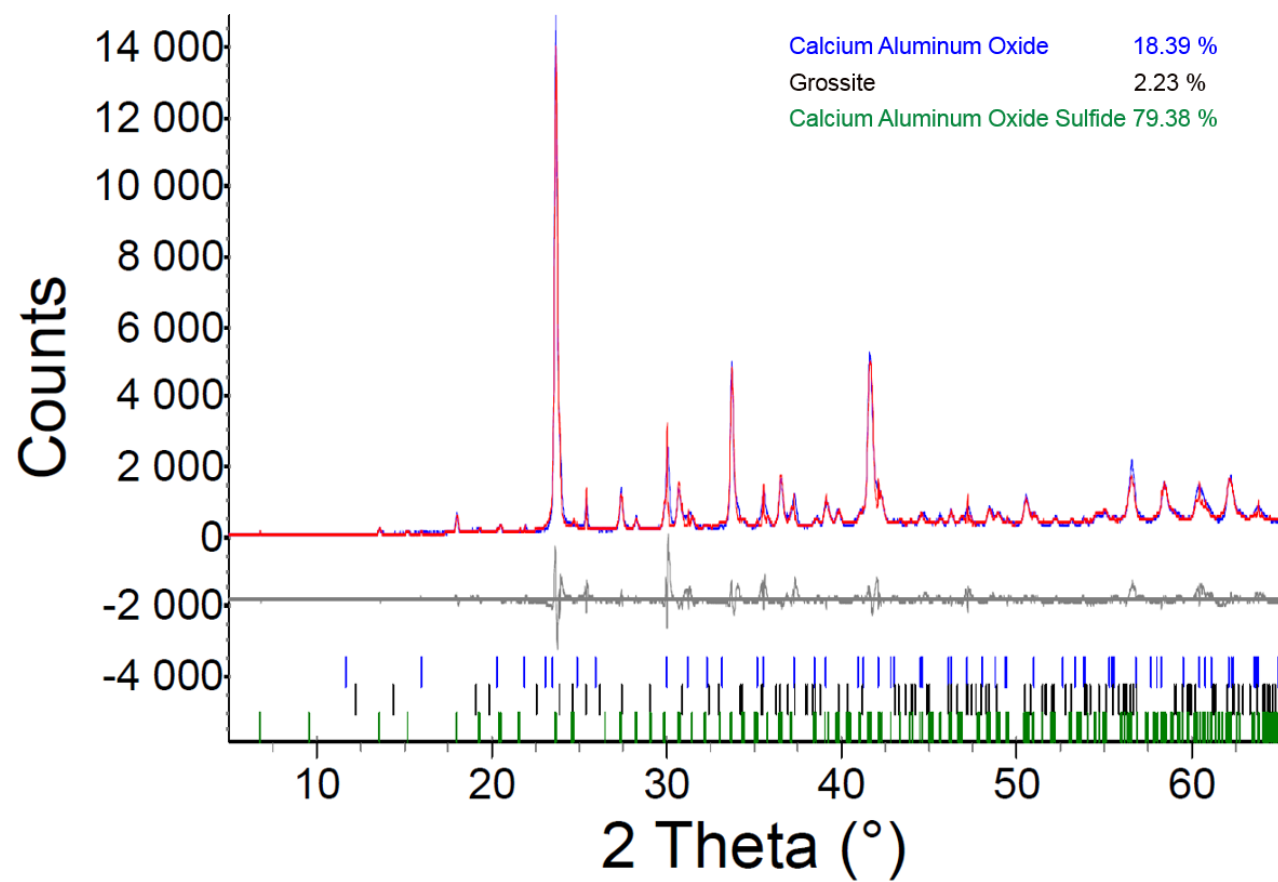


Figure 6-a

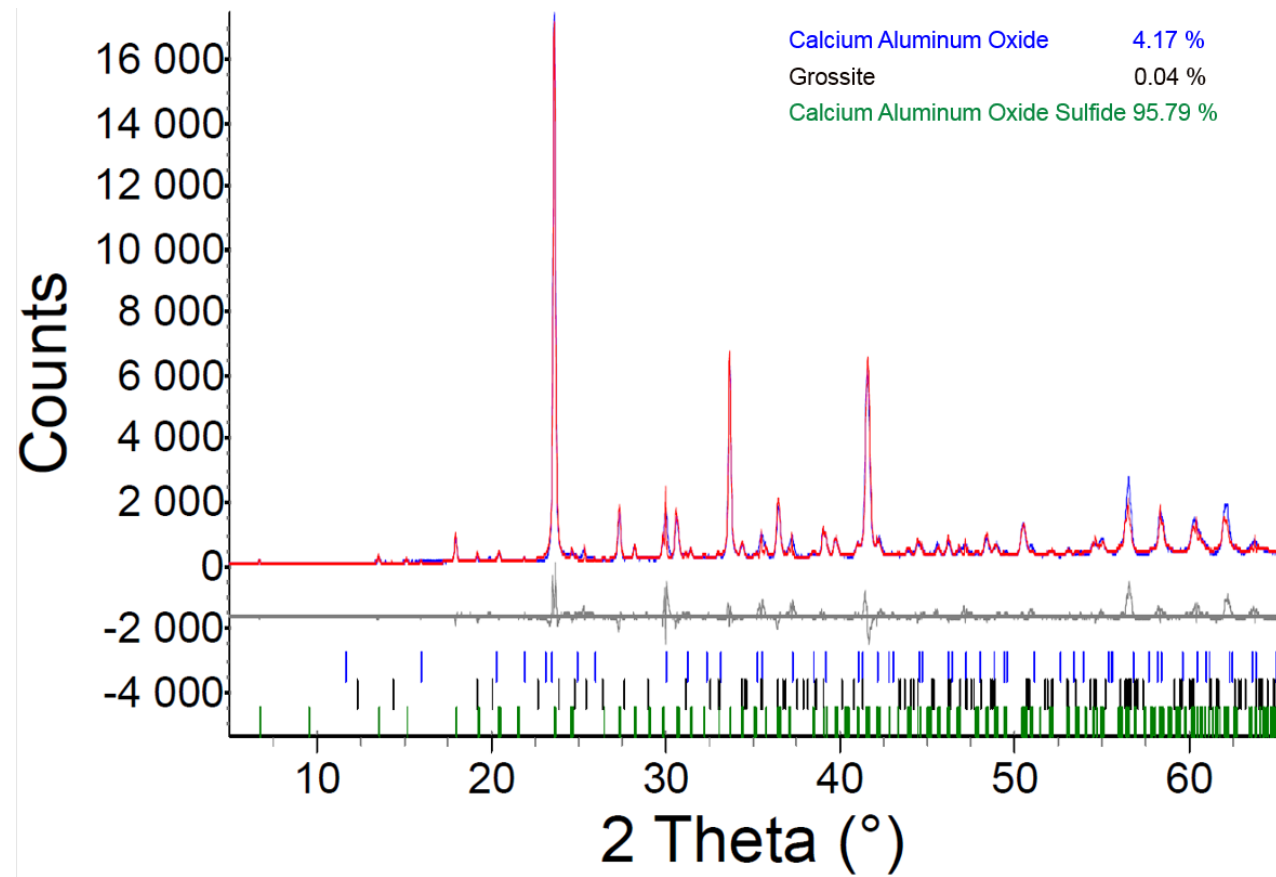


Figure 6–b

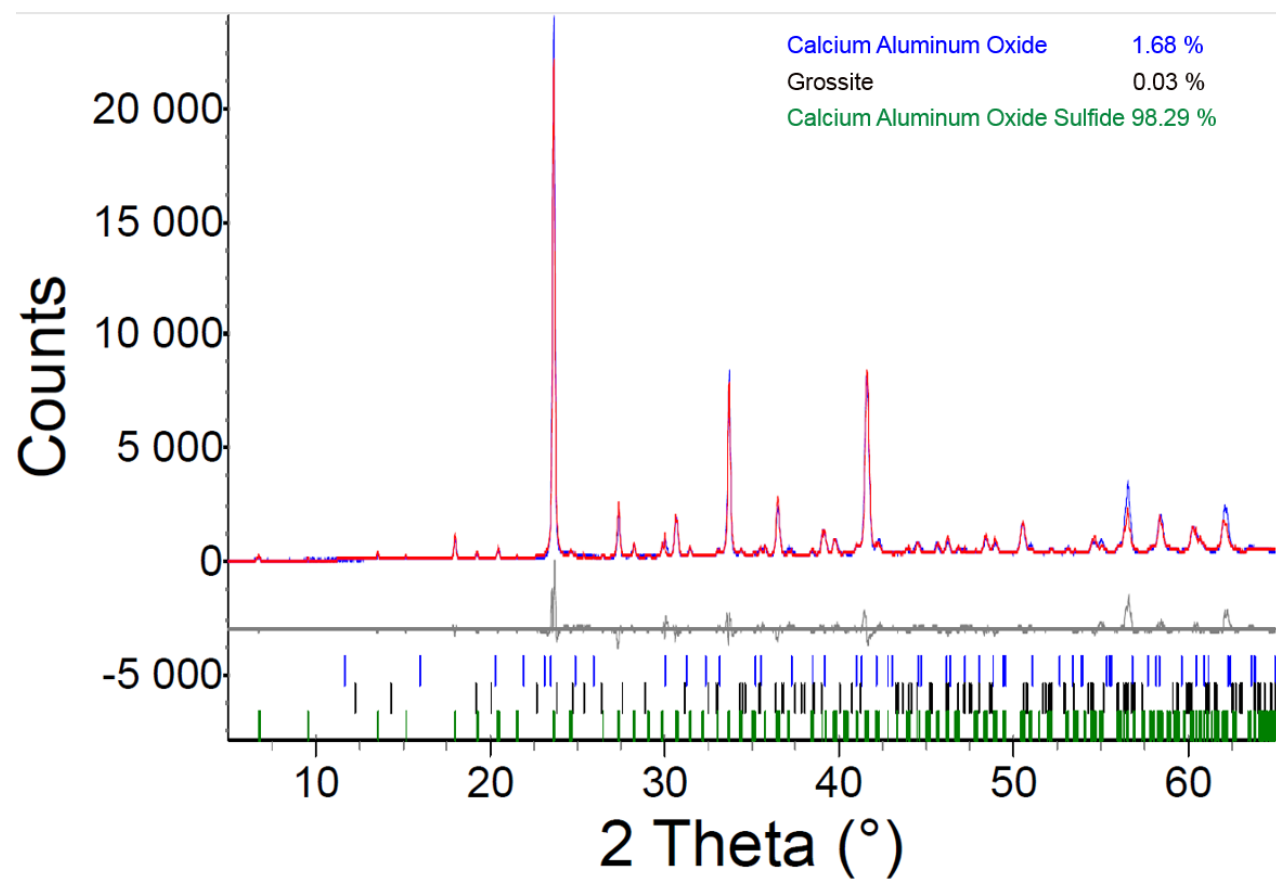


Figure 6–c

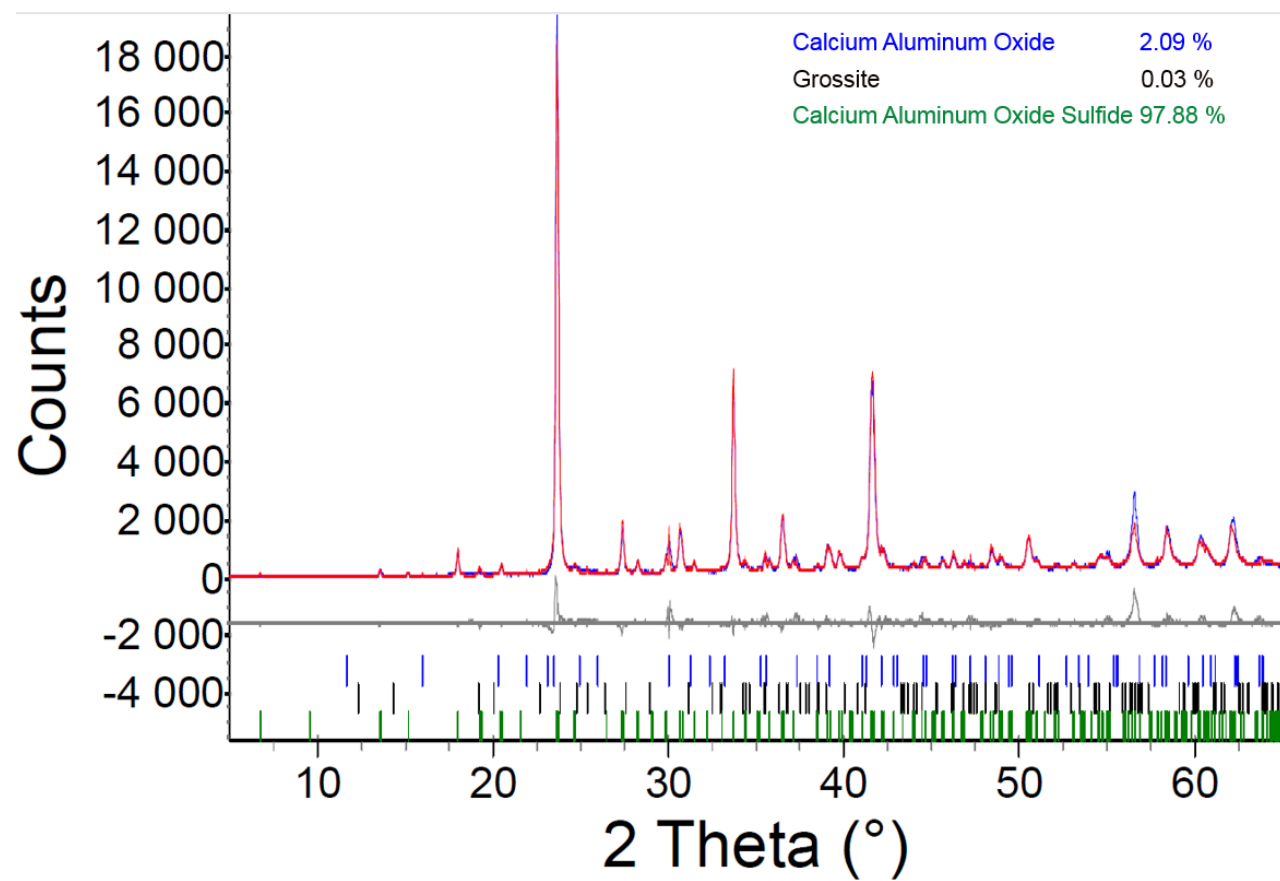


Figure 6-d

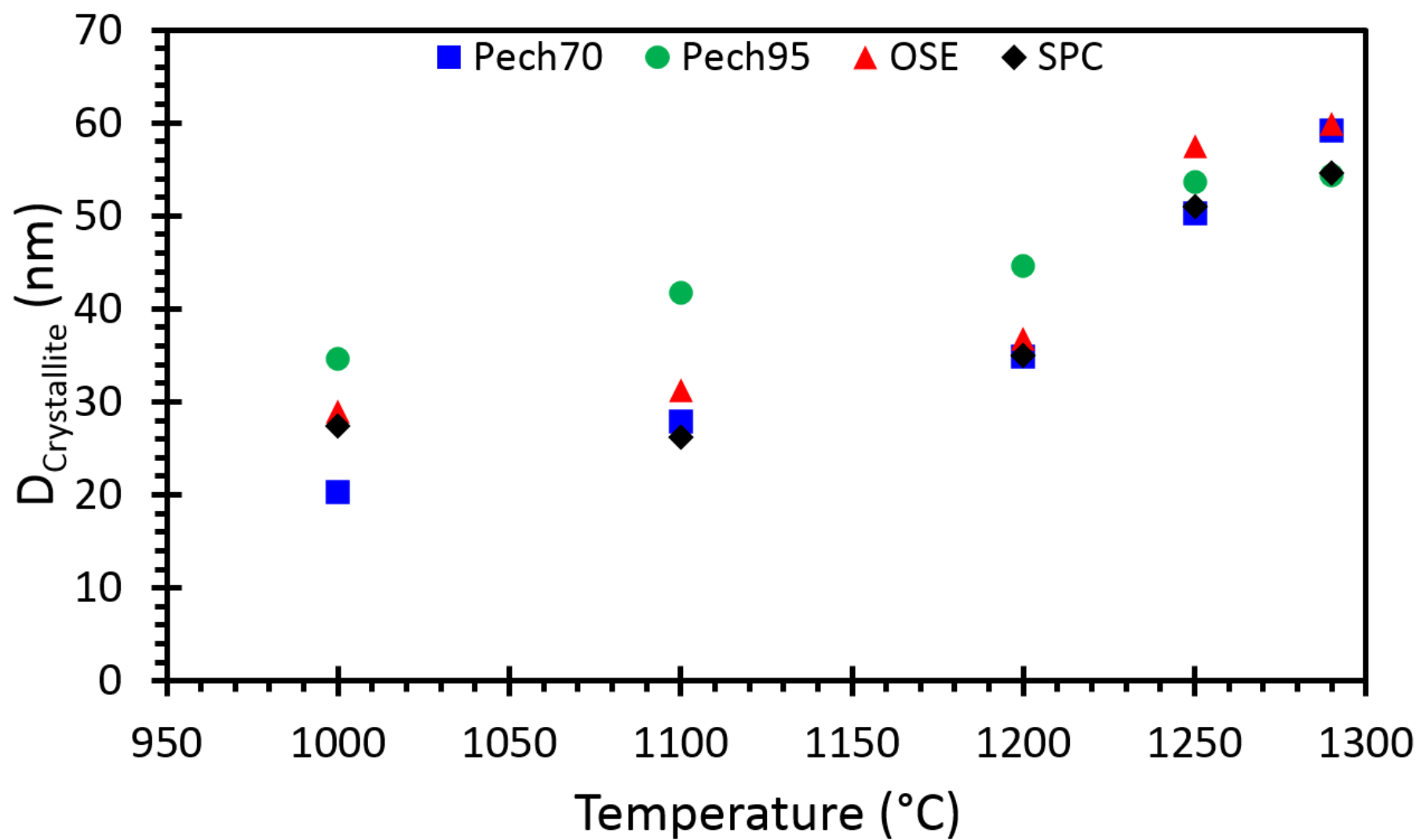
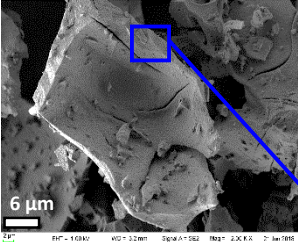
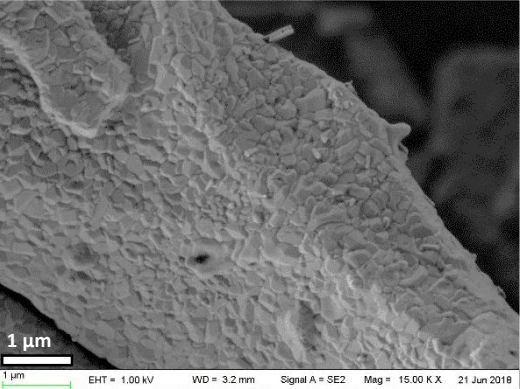
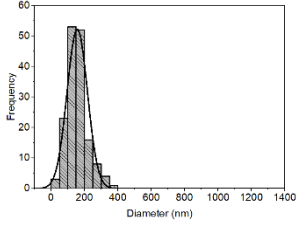
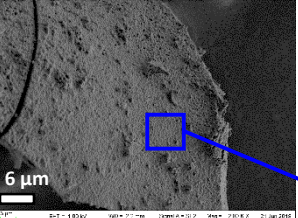
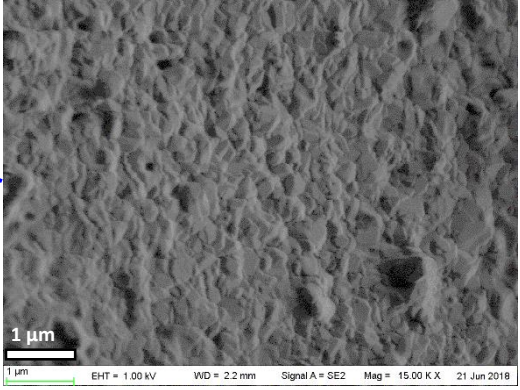
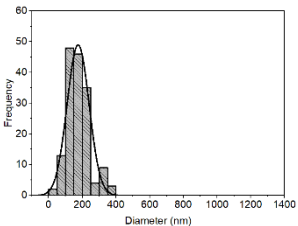
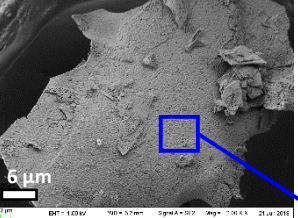
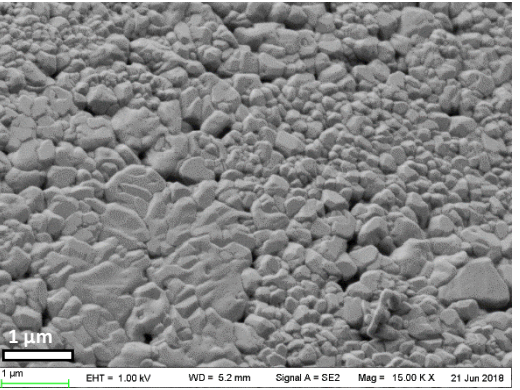
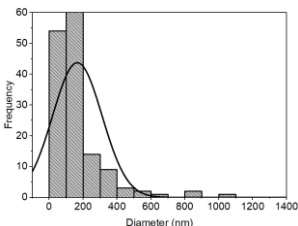


Figure 7

Samples treated at 1250 °C with statistical parameters of PSD-IA	
Pech70 method	   <p><math>N_{total} = 160</math> ; Mean size = 157 nm ; Standard Deviation = 61 nm</p>
Pech95 method	   <p><math>N_{total} = 160</math> ; Mean size = 175 nm ; Standard Deviation = 65 nm</p>
OSE method	   <p><math>N_{total} = 160</math> ; Mean size = 166 nm ; Standard Deviation = 146 nm</p>



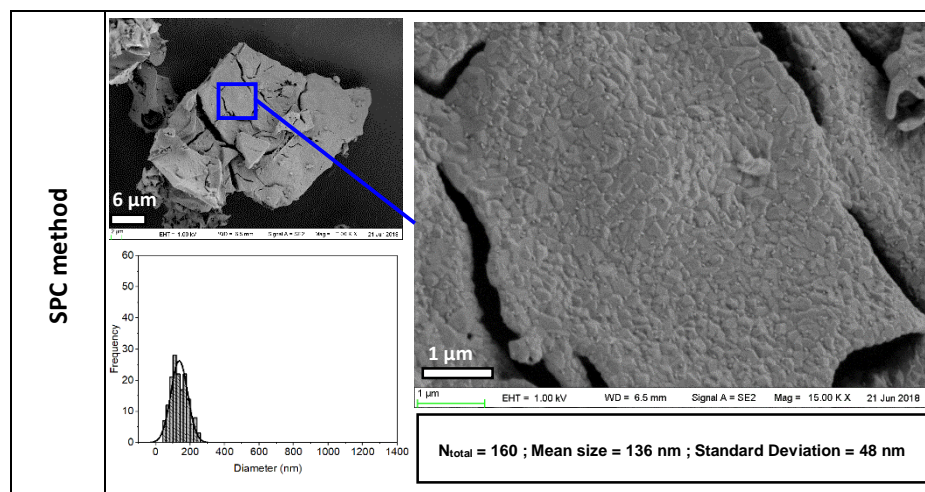


Figure 8

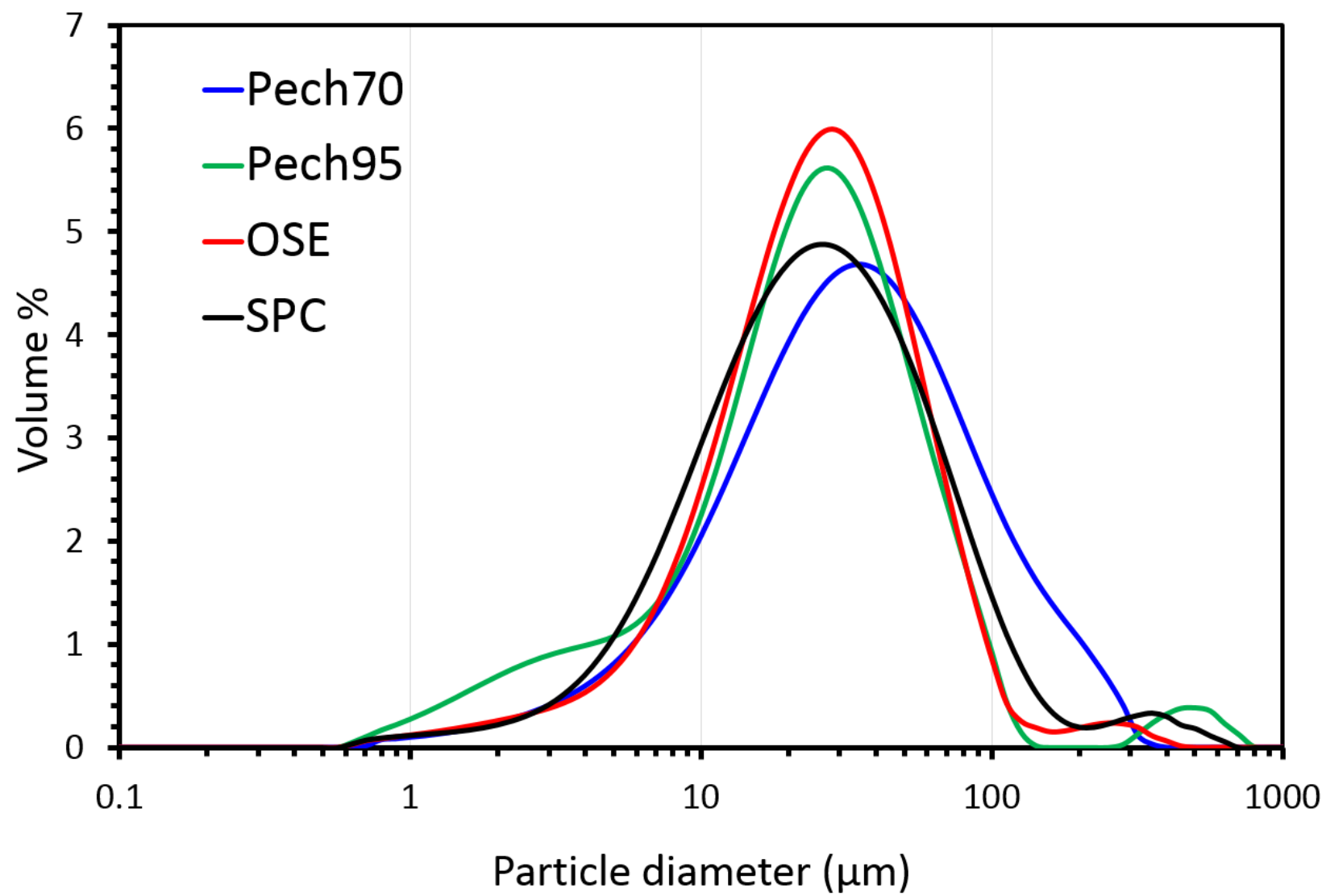


Figure 9

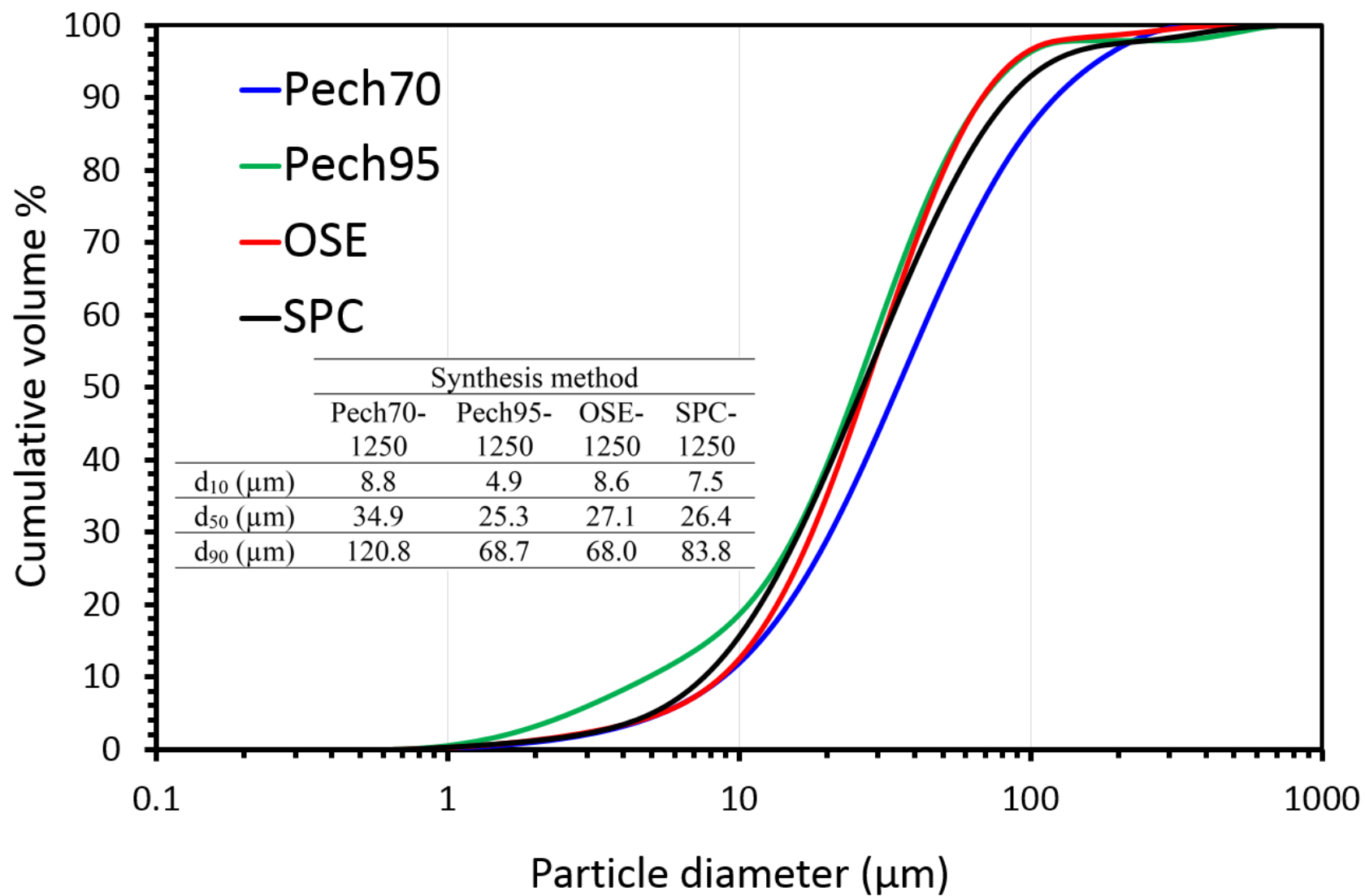


Figure 10

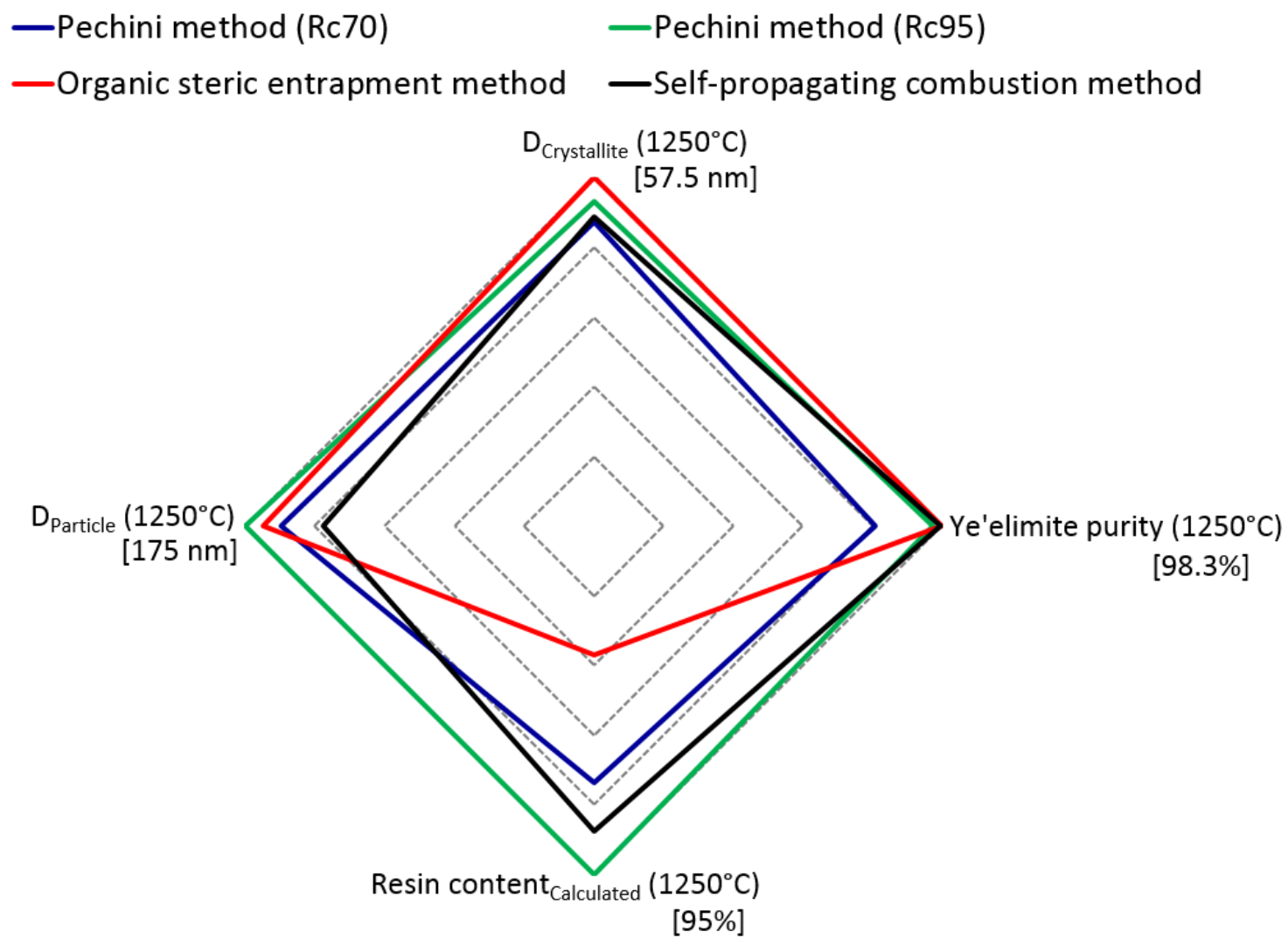


Figure 11

## Table captions

Table 1	Summary of physical and chemical characteristics of some cementitious phases prepared by chemical synthesis routes (Pech=Pechini method; OSE=Organic Steric Entrapment method; SPC=Self-Propagating Combustion).
Table 2	Powder preparation and processing variables.
Table 3	Comparison between the principles of the three chemical routes used in the present work for synthesis of ye'elinite.
Table 4	ICSD collection codes for all phases used for Rietveld refinements.
Table 5	Summary of thermal events shown in Fig. 4.
Table 6	Quantitative Rietveld analysis of the powders prepared by Pech70, Pech95, OSE and SPC routes after a heat treatment from 1000 °C to 1250 °C for 1 h. The values in brackets correspond to phase content error from Rietveld quantitative analysis. (*) Rwp is the weighted profile factor.

**Table 1**

	Cementitious phases													
	$C_4A_3\bar{S}$	$C_3S$			$C_2S$					CA				
Reference	[9]	[10]	[16]	[20]	[10]	[12]	[13]	[14]	[15]	[17]	[11]	[21]	[18]	[19]
Chemical method	OSE	OSE	SPC	Sol-gel	OSE	Pech	Pech	Pech	Pech	SPC	Pech or SPC	Pech	SPC	SPC
Grain size (nm)	-	200-300	-	-	80-90	-	-	-	-	45	50	-	-	-
Specific surface area (m <sup>2</sup> /g)	1-2.5	50	-	-	22.1	8.3	1-30	0.8-3.1	1-22	-	-	10	-	-
Purity	Pure	-	Not pure	Pure	-	Pure	Pure	Pure	Pure	Pure	Pure	Pure	Pure	Not pure
Purity verification method	XRD pattern	XRD pattern	XRD pattern	XRD pattern	XRD pattern	XRD pattern	XRD pattern	XRD pattern	XRD pattern	XRD pattern	XRD pattern	XRD pattern	Rietveld method	XRD pattern

**Table 2**

Chemical synthesis route	Chemical reactants	Content (g or ml)	pH of the solution	Solution color	Visual aspect of the dried gel (Fig. 1)
Pechini method (Rc70%)	Ca(NO <sub>3</sub> ) <sub>2</sub> ·4H <sub>2</sub> O	3.095 g	4.13	Transparent	Brown gel, fairly coarse texture
	Al(NO <sub>3</sub> ) <sub>2</sub> ·9H <sub>2</sub> O	6.557 g			
	Al <sub>2</sub> (SO <sub>4</sub> ) <sub>3</sub> ·16H <sub>2</sub> O	0.688 g			
	Deionized H <sub>2</sub> O	30 ml			
	Citric acid	2.8 g			
Pechini method (Rc95%)	Ethylene glycol	1.68 ml	1.93	Transparent	Black gel, soft and porous texture
	Ca(NO <sub>3</sub> ) <sub>2</sub> ·4H <sub>2</sub> O	3.095 g			
	Al(NO <sub>3</sub> ) <sub>2</sub> ·9H <sub>2</sub> O	6.557 g			
	Al <sub>2</sub> (SO <sub>4</sub> ) <sub>3</sub> ·16H <sub>2</sub> O	0.688 g			
	Deionized H <sub>2</sub> O	30 ml			
Organic steric entrapment method	Citric acid	22.8 g	5.8	Transparent	White gel, coarse texture
	Ethylene glycol	13.69 ml			
	Ca(NO <sub>3</sub> ) <sub>2</sub> ·4H <sub>2</sub> O	3.095 g			
	Al(NO <sub>3</sub> ) <sub>2</sub> ·9H <sub>2</sub> O	6.557 g			
	Al <sub>2</sub> (SO <sub>4</sub> ) <sub>3</sub> ·16H <sub>2</sub> O	0.688 g			
Self-propagating combustion method	Deionized H <sub>2</sub> O	30 ml	3.62	Transparent	Dark brown gel, soft and porous texture
	PVA 22000 (5 mass% aqueous sol.)	1.11 g			
	Ca(NO <sub>3</sub> ) <sub>2</sub> ·4H <sub>2</sub> O	3.095 g			
	Al(NO <sub>3</sub> ) <sub>2</sub> ·9H <sub>2</sub> O	6.557 g			
	Al <sub>2</sub> (SO <sub>4</sub> ) <sub>3</sub> ·16H <sub>2</sub> O	0.688 g			
	Deionized H <sub>2</sub> O	30 ml			
	Citric acid	10 g			

**Table 3**

Chemical route	Pechini synthesis	Organic steric entrapment	Self-propagating combustion
Symbol	PECH	OSE	SPC
Raw materials	Citric acid + ethylene glycol + dissolved salts	Polyvinyl alcohol + dissolved salts	Citric acid + dissolved salts
Organic medium	Polyester	PVA chain	Citric acid
Resin content Rc % (calculated from equation (1))	Rc (Pech70) = 70 % Rc (Pech95) = 95 %	Rc (OSE) = 35 %	Rc (SPC) = 83 %



**Table 4**

Phase name	Cementitious notation	Chemical formula	ICSD codes	Ref.
Orthorhombic ye'elimite	orth- $C_4A_3\bar{S}$	$Ca_4Al_6O_{16}S$	80361	[33]
Krotite	CA	$CaAl_2O_4$	260	[34]
Grossite	$CA_2$	$CaAl_4O_7$	34487	[35]
Lime	C	CaO	52783	[36]
Calcium carbonate	$C\bar{C}$	$CaCO_3$	73446	[37]
Anhydrite	$C\bar{S}$	$CaSO_4$	15876	[38]
Bassanite	$C\bar{S}H_{0.5}$	$2CaSO_4 \cdot H_2O$	79529	[39]

**Table 5**

Chemical route	Stage	Temperature range	Thermal event		Possible phenomena
			TGA	TDA	
Pech70	I	30 - 200 °C	-1 %	Endo.	Evaporation of residual water
	II	370 - 750 °C	-8 %	Exo.	Organic phase combustion
	III	860 - 950 °C	~ 0 %	Exo.	Phase crystallization
	IV	950 - 1000 °C	-0.7 %	Exo.	Residual carbon combustion
Pech95	I	30 - 200 °C	-0.9 %	Endo.	Evaporation of residual water
	II	300 -700 °C	-7.5 %	Exo.	Organic phase combustion
	III	850 - 940 °C	~ 0 %	Exo.	Phase crystallization
	IV	940 - 1000 °C	-0.1 %	Exo.	Residual carbon combustion
OSE	I	30 - 200 °C	-0.3 %	Endo.	Evaporation of residual water
	II	400 - 650 °C	-2.1 %	Endo.	Breakdown of the polymer chains
	III	850 - 950 °C	-0.4 %	Exo.	Residual carbon combustion
	IV	950 - 1000 °C	~ 0 %	Exo.	Phase crystallization
SPC	I	30 - 200 °C	-1.6 %	Endo.	Evaporation of residual water
	II	400 -750 °C	-7.4 %	Exo.	Organic phase combustion
	III	750 - 855 °C	~ 0 %	Exo.	Phase crystallization
	IV	900 - 1000 °C	-1 %	Exo.	Residual carbon combustion

**Table 6**

Temperature of heat treatment (°C)	Synthesis method	Crystalline phases			Fitting parameters of Rietveld analysis Rwp <sup>(*)</sup>
		Orth- C <sub>4</sub> A <sub>3</sub> $\bar{S}$ (wt%)	CA (wt%)	CA <sub>2</sub> (wt%)	
1000	Pech70 method	55.2 (1.5)	17.9 (1.2)	26.9 (1.1)	12.52
	Pech95 method	37.1 (1.3)	41.1 (1.2)	21.7 (1.1)	13.54
	OSE method	64.9 (1.2)	22.5 (1.1)	12.6 (0.7)	8.65
	SPC method	58.1 (1.6)	24.9 (1.4)	16.9 (1.0)	9.77
1100	Pech70 method	63.7 (1.4)	21.2 (1.3)	15.1 (0.8)	13.04
	Pech95 method	48.9 (1.0)	32.2 (0.9)	18.9 (0.8)	12.11
	OSE method	68.4 (1.1)	17.3 (0.9)	14.3 (0.8)	8.79
	SPC method	59.6 (1.8)	21.3 (1.6)	19.0 (0.9)	10.52
1200	Pech70 method	62.1 (1.2)	23.2 (1.1)	14.7 (0.8)	12.62
	Pech95 method	57.3 (1.0)	26.6 (0.8)	16.2 (0.9)	10.96
	OSE method	78.7 (0.9)	12.2 (0.7)	9.0 (0.8)	7.85
	SPC method	57.3 (1.2)	26.4 (0.9)	16.2 (0.9)	10.96
1250	Pech70 method	79.4 (0.5)	18.4 (0.3)	2.2 (0.3)	12.63
	Pech95 method	95.8 (0.4)	4.2 (0.3)	0 (0.3)	10.65
	OSE method	98.3 (0.3)	1.7 (0.2)	0 (0.2)	11.45
	SPC method	97.9 (0.2)	2.1 (0.1)	0 (0.1)	12.02
1290	Pech70 method	78.9 (0.5)	18.2 (0.3)	2.9 (0.4)	18.14
	Pech95 method	92.6 (0.4)	7.4 (0.3)	0 (0.3)	17.01
	OSE method	97.5 (0.3)	2.4 (0.2)	0 (0.2)	15.28
	SPC method	96.9 (0.2)	3.1 (0.1)	0 (0.2)	13.80